Medical Image Analysis 13 (2009) 634–649

Contents lists available at ScienceDirect

Medical Image Analysis

journal homepage: www.elsevier.com/locate/media

Fractal and multifractal analysis: A review

R. Lopes [a,b], N. Betrouni [a,*]

[a] Inserm, U703, Pavillon Vancostenobel, CHRU Lille, Lille Cedex 59037, France
[b] Laboratoire d'automatique LAGIS, CNRS UMR 8146, USTL, Bâtiment P2, Villeneuve d'Ascq 59655, France

ARTICLE INFO

Article history:
Received 8 November 2007
Received in revised form 1 April 2009
Accepted 15 May 2009
Available online 27 May 2009

Keywords:
Fractal analysis
Fractal dimension
Multifractal analysis
Multifractal spectrum
Texture
Characterization

ABSTRACT

Over the last years, fractal and multifractal geometries were applied extensively in many medical signal (1D, 2D or 3D) analysis applications like pattern recognition, texture analysis and segmentation. Application of this geometry relies heavily on the estimation of the fractal features. Various methods were proposed to estimate the fractal dimension or multifractal spectral of a signal. This article presents an overview of these algorithms, the way they work, their benefits and their limits. The aim of this review is to explain and to categorize the various algorithms into groups and their application in the field of medical signal analysis.

1. Introduction

The idea of describing natural phenomena by studying statistical scaling laws is not recent. Indeed, many studies were carried out on this topic (Bachelier, 1900; Frish, 1995; Kolmogorov, 1941; Mandelbrot, 1963). However, there has been a recent resurgence of interest in this approach. A great number of physical systems tend to present similar behaviours on different scales of observation. In the 1960s, the mathematician Benoît Mandelbrot used the adjective "fractal" to indicate objects whose complex geometry cannot be characterized by an integral dimension.

The main attraction of fractal geometry stems from its ability to describe the irregular or fragmented shape of natural features as well as other complex objects that traditional Euclidean geometry fails to analyse. This phenomenon is often expressed by spatial or time-domain statistical scaling laws and is mainly characterized by the power-law behaviour of real-world physical systems. This concept enables a simple, geometrical interpretation and is frequently encountered in a variety of fields, such as geophysics, biology or fluid mechanics. To this end, Mandelbrot introduced the notion of fractal sets (Mandelbrot, 1977), which enables to take into account the degree of regularity of the organizational structure related to the physical system's behaviour.

Fractal geometry is widely used in image analysis problems in general and especially in the medical field. It is applied in different ways with different results. However, there has been no review paper to digest these different methods and their application. The purpose of this paper is to provide a survey of these methods and to discuss the principal results. This research may provide assistance to researchers aiming to use this geometry in medical imaging applications. It is organised as follow: in the next section, we introduce more formally the fractals; Section 3 discusses the relevance of fractals in image analysis. Section 4 gives the survey of the methods, their principles and limitations. Sections 5 and 6 are respectively reserved to multifractal analysis and the associated algorithms. Section 7 discusses the main applications of fractals/multifractals in the medical image analysis procedures and the methods used.

2. Fractals and dimensions

A definition that can illustrate the notion of fractal can be as follows: consider an object. One has to take an element of this object. One has to surround it with a sphere of a given radius R and count the amount of object elements Σ inside the sphere. The measure of Σ can be arbitrary. Here, of importance is only the dependence of Σ on the sphere radius after averaging over the element put in its origin. This definition takes into account the fact that the relevant dimension of an object depends on the spatial scale.

A fundamental characteristic of fractal objects is that their measured metric properties, such as length or area, are a function of the scale of measurement. A classical example to illustrate this property is the "length" of a coastline (Mandelbrot, 1967). When measured at a given spatial scale d, the total length of a crooked coastline $L(d)$ is estimated as a set of N straightline segments of

* Corresponding author. Tel.: +33 320 446 7 22; fax: +33 320 446 715.
E-mail address: n-betrouni@chru-lille.fr (N. Betrouni).

1361-8415/$ - see front matter © 2009 Elsevier B.V. All rights reserved.
doi:10.1016/j.media.2009.05.003

length d. Because small details of the coastline not recognized at lower spatial resolutions become apparent at higher spatial resolutions, the measured length $L(d)$ increases as the scale of measurement d increases. Thus, in fractal geometry, the Euclidean concept of "length" becomes a process rather than an event, and this process is controlled by a constant parameter (Fig. 1).

More formally, Mandelbrot (1983) defined a fractal set as a set for which the Hausdorff dimension (D_h) is greater than its topological dimension (D_T). With:

The Hausdorff–Besicovitch dimension D_h is defined as the logarithmic ratio between the number N of an object's internal homotheties and the reciprocal of the common ratio r of this homothety:

$$D_h = \frac{\ln(N)}{\ln\left(\frac{1}{r}\right)} \quad (1)$$

The homothety term could be associated to a reduction term. For example, a fractal respecting Eq. (1) will be constituted of N patterns of which the size has been reduced of a factor r (for homothety).

The topological dimension D_T (defined by recurrence) of an object corresponds to the number of independent variables needed to describe it. Thus, a point has a 0-dimensional, a curve has a 1-dimensional, a plane has a 2-dimensional, and in general euclidean space R^n has n-dimensional.

Still according to Mandelbrot (1967), analytically, the relationship between the measuring scale δ and the length L can be expressed as:

$$L(\delta) = K \cdot \delta(1 - D) \quad (2)$$

where K is a constant and D is known as the fractal dimension, a non integer number (fractional). It is the main tool used to describe the fractal geometry and the heterogeneity of irregular shapes. It allows capturing what is lost in traditional geometrical representation of shapes. In Euclidean geometry, topological dimensions (D_T) of forms remain constant and do not provide detail about the irregularity of the form. For instance, in 1D, D_T is unable to distinguish a straight line and a crooked line.

From another side, fractals are considered as self-similar objects. This last feature is a key issue in fractals. It implies that the object looks similar to its zoomed part. Formally, self-similarity is defined as a property where a subset, when magnified to the size of the whole, is indistinguishable from the whole (Mandelbrot, 1967).

In the same context, fractals are said self-affine if the variation in one direction scales differently than the variation in another direction (Mandelbrot, 1985). Whereas, self-similar objects are isotropic.

3. Fractals and image analysis

The diagnostic interpretation of medical images is a multi-steps task where the aim is the detection of potential abnormalities. This goal is accurately achieved when the clinician integrates two processes. The first is the image perception to recognize unique image patterns and the second is the identification of the relationship between perceived patterns and possible diagnoses. The success of these two steps relies heavily on the clinician skill. One of the used features in this process is texture which is a rich source of visual information and is a key component in image analysis and understanding in humans. Texture is known to provide cues about scenic depth and surface orientation and, as such, describes the content of both natural and artificial images. Also, there is evidence of perceptual learning in texture-coding mechanisms and in textural discrimination (Tourassi, 1999).

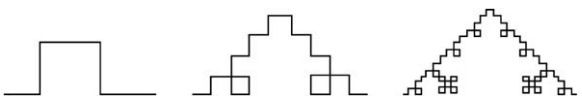

Fig. 1. The first iterations to build a fractal structure.

In light of this, many studies were conducted to develop algorithms that can quantify the textural properties of an image. However, the exciting evolution of both texture analysis algorithms and computer technology revived researchers' interest in applications for medical imaging in recent years. During the past decade, results from numerous published articles have shown the ability of texture analysis algorithms to extract diagnostically meaningful information from medical images that were obtained with various imaging modalities, such as chest radiography, mammography, ultrasound (US), computed tomography (CT), single photon emission computed tomography (SPECT), positron emission tomography (PET) and magnetic resonance imaging (MRI).

The applicability and the relevance of fractal geometry in medical image analysis is justified by the fact that self-similarity can hardly be verified in biological objects imaged with a finite resolution. Indeed, the images are not only spectrally and spatially complex, but they often exhibit certain similarities at different spatial scales. This assertion induces that spatially complex patterns could be described by simple texture features. In fact, the problem of features definition for texture analysis in image understanding and pattern recognition was an increasing research domain for many years (Haralick et al., 1973; Pratt et al., 1978). Precisely, fractal geometry offers the ability to describe and to characterize the complexity of the images or more precisely of their texture composition.

4. Fractal dimension computing methods

When applied in image analysis, fractal geometry is often brought to the evaluation of the fractal dimension (referred to as FD or D). Many methods exist to compute this dimension; each method has its own theoretic basis. This fact often leads to obtain different dimensions by different methods for the same feature. These differences appear because the Hausdorff–Besicovitch dimension (Eq. (1)) is not computable in this form in most cases. Thus, the methods approximate it using different algorithms to estimate the parameter N.

Although, the applied algorithms differ, they obey to the same basis summarized by the three steps:

- Measure the quantities of the object using various step sizes.
- Plot log (measured quantities) versus log (step sizes) and fit a least-squares regression line through the data points.
- Estimate FD as the slope of the regression line.

In the next paragraph, we present and classify the most widespread literature methods grouped into three classes: box-counting methods; fractional Brownian motion (fBm) methods, and area measurement methods.

The first methods were the box-counting methods. In these methods the signals are represented on a finite scale grid and the grid effects interplayed with the computing fractal dimension. For this reason, other methods have been defined to remove the grid effects such as the fBm methods.

4.1. Box-counting methods

Methods in this class share the following steps: each algorithm requires a meshing of the signal, formulation of a probability in

each generated box and the estimation of the FD by a least-squares linear fitting as last step. The box-counting methods have been the first methods to compute the FD of a signal. Their principles were simple and easy to develop, but, as it will be shown below, they present some drawbacks.

4.1.1. Box-counting method (BC)

This method was defined by Russel et al. (1980), it is the most frequently used and most popular method. By covering a binary signal with boxes of length r, the FD is estimated as:

$$\mathrm{FD} = -\lim_{r\to 0}\frac{\log(N(r))}{\log(r)} \tag{3}$$

where $N(r)$ is number of boxes needed to completely cover the signal.

This method has many limitations because it requires signal binarization. Later on, Normant and Tricot (1991) showed that this method is not theoretically well founded and is valid only for statistically self-similar signals.

Moreover, as the reiteration for different sizes of r can produce various sizes of N_r, the grid should be randomly relocated at each iteration (Appleby, 1996). More recently, Pruess (2007) showed that the computation of the FD is box size sensitive.

Always in the box-counting methods class, the compass method defined by Mandelbrot (1983) and the yardstick method defined by Sanderson and Goulding (1990) in 1990 presented the same drawbacks.

4.1.2. Differential box-counting method (DBCM)

Differential box-counting method (DBCM) is an adaptation of the box-counting method. It was proposed by Chaudhuri and Sarkar (1995) to solve some of limitations of the BM method. It has the advantage to work on grey-scale images and thus the binarization step is avoided. The signal is partitioned into boxes of various size r and $N(r)$ is computed like the difference between the minimum and the maximum grey levels in the (i,j)th box. This step is repeated for all boxes and the FD is estimated as in Eq. (3).

An important limit of the box-counting methods is the choice of the box size. Many studies were done to find the upper and lower bounds for the box size and in this regard (Chen et al., 1993) proposed a theoretical justification for a restriction on the smallest box size inspired by the work of Pickover and Khorasani (1986). Also Bisoi and Mishra (2001) established a lower bound of the box size to ensure accurate results. They showed that, with a too low box size, the maximum number of boxes above the grid would be more than the number of available intensity levels. The resulting unaccounted boxes would lead to an underestimation of FD. In the same manner, for a too high box size, the number of boxes would be much less than the number of intensity levels.

Asvestas et al. (1998) showed that this method was not numerically stable. Indeed they tested this method on a set of images generated by the random midpoint displacement method. They highlighted the fact that the method underestimates the true value of FD.

Improvements of the "differential box-counting" method are described in (Biswas et al., 1998; Jin et al., 1995).

4.1.3. "Extended counting" method (XCM)

The extended counting method "XCM" (Sandau and Kurz, 1997) was proposed as an alternative to the BCM. The principle of the XCM can be formulated as follows: The BCM is applied to many subsets of a fractal set and the maximum of the subsets' dimensions is taken as the FD of the set. On the other hand, the BCM, as it is used for subsets, it is extremely simplified (a box-counting regression line is built only on the basis of two points).

This method can be compared to the BCM because the FD is computed on binary signals. Although the BCM is the most widespread, Sandau and Kurz (1997) showed that the XCM presents some benefits. Indeed, XCM, in contrast to BCM, calculates a measure of complexity without regression. Hence, this measure grows monotonously with complexity and is determined by the most complex region of the signal. This corresponds to an important feature of FD, the maximum property, which is approximately fulfilled by XCM, but not by BCM. Also, XCM is less sensitive to the signal rotation and translation influence.

The drawbacks of this method are that it can only be applied to binary signals. Hence, it is often used to compute the FD of a skeletonized image (Chung et al., 2002). Moreover XCM has tendency to overestimate the FD. Finally, Prigarin et al. (2008) tested XCM on fractional Brownian signals and concluded that the XCM is not suitable for these signals.

4.2. Fractional Brownian motion (fBm) methods

The fractal model based on fBm is a non-stationary model and is often used to describe random phenomenon. Pentland (1984) showed that most fractals encountered in physical models are fractal Brownian functions (fBfs). An fBf (Mandelbrot, 1975) f is a generalization of Brownian motion where the expected value of the intensity difference between two points is zero but where the square of the difference is proportional to the distance between the points at a power $2H$.

The FD of an n-dimension fBf is defined by:

$$\mathrm{FD} = n + 1 - H \tag{4}$$

Fractal Brownian functions are statistically self-affine (Mandelbrot, 1983). It follows that linear transformations and scalings of a fBf do not affect its FD. With this formalism, the FD of a fractal Brownian function is invariant with transformations.

Two algorithms are commonly used to estimate the FD of an image considered to be a 2D fractal Brownian function. They are based either on the variogram or the Fourier transform of the image.

4.2.1. Variogram method

The variogram method is based on the statistical Gaussian modelling of images. Given a FD, it is possible to use fractional Brownian motion modelling to create a corresponding image. This method attempts to solve the inverse problem: given an image, the FD is estimated by assuming that it is derived from a fractional Brownian motion (Goodchild, 1980).

This algorithm provides robust estimations of the FD (Soille and Rivest, 1996). Indeed the advantages of the variogram method are its applicability to irregularly distributed data sets and to surfaces with an underlying trend, as commonly occur in topography. For surfaces with a trend of higher than linear order, the residual variogram is preferable. Although the theoretical derivation assumes second-order stationarity, the surface does not need to be stationary to use the variogram method. However it was shown that dividing a signal into an insufficient number of clusters makes the variogram method enable to estimate the FD, but when a sufficient large number of clusters is used it is possible to detect a very sharp drop toward the correct value, followed by slow convergence (Kolibal and Monde, 1998).

On the other hand, the variogram method yields accurate results only for low dimensions surfaces. For higher dimensions surfaces, the method is unstable (Lam et al., 2002).

4.2.2. The power spectrum

Power spectrum method (Pentland, 1984) is based on the power spectrum dependence of fractional Brownian motion. In this

method, each image line is Fourier transformed, the power spectrum is evaluated and then all these power spectra are averaged. FD is computed as the slope.

The Fourier method is ideal for the self-affine surfaces analysis and for simulation. Unfortunately, the method is slow and requires gridded data. The radial calculation scheme works only for isotropic surfaces.

Asvestas et al. (1998) defined a modified version to estimate the FD of a two variable fBm functions from its average power spectrum. The method is called Power Differentiation method. The authors showed that their method is more robust in the presence of white noise.

The main drawback is that the method is efficient only with surfaces exhibiting an exponential power spectrum. In general, this restriction imposed on the shape of the power spectrum is not valid and this may cause errors in the calculation of FD (Osborne and Provenzale, 1989).

4.3. Area measurement methods

Area measurement methods use structuring elements (triangle, erosion, dilatation, ...) of various scales r and compute the area $A(r)$ of the signal intensity surface at scale r. The FD is obtained by the slope of the best fitting line at the points $(\log(r), \log(A(r)))$. In this methods class, three algorithms are the most used:

4.3.1. Isarithm method (IM)

The idea of the isarithm method (Shelberg et al., 1983) is to define the complexity of isarithm or contour lines, needed to approximate the complexity of a surface. This method is only defined for the 2D case. A series of isarithms (e.g., contours) based on the data values are formed on the image. The FD of each isarithm can be estimated with the walking divider method and the FD of the image is the average FD of the isarithms plus one.

Shelberg et al. (1983) showed that the method can be used to estimate the FD for the non self-similar surfaces. It is an important key, because others methods, like BCM, are only appropriate for self-similar surfaces. Furthermore, the method was found to be robust to random noise (Qiu et al., 1999).

However, Lam and De Cola (2002) noted that real data are generally anisotropic and therefore the computed FD will vary depending on whether it is measured along rows, columns, or in a non-cardinal direction. Moreover, conflicting results on the performance of the isarithm method have been reported. Lam et al. (1997) found that the isarithm method performed well in returning FD values close to those of true surface dimensions, whereas Klinkenberg and Goodchild (1992) found results with this method to be poor. Clarke (1986) criticized the isarithm method because the resulting dimension was likely to depend on the values of the isarithms and isarithm interval.

4.3.2. Blanket method (BM)

The blanket algorithm was originally devised by Peleg et al. (1984) in order to calculate the area of a gray level surface and thus the FD of a 3D structure. The algorithm is based upon Mandelbrot's method and ultimately upon Minkowski's sausage logic. In the algorithm, Peleg et al. considered all the points in 3D space at a distance ε from the surface, covering the surface with a "blanket" of thickness 2ε. This blanket is defined by two surfaces, an upper surface and a lower surface (defined by dilatation and erosion of the image).

One of the advantages of the method is it robustness against gray levels changes. Another benefit is that the use of asymmetric structuring elements allowed the identification of anisotropic structures within the image (Chappard et al., 2001).

Asvestas et al. (1998) showed that the BM is efficient only when the theoretical value of the FD is relatively low. Experiments were done one noise free and noised data. For the first case, the method underestimated the high FD and for the second case, it underestimated the low FD.

4.3.3. Triangular prism method (TPM)

The triangular prism method compares the surface areas of triangular prisms with the pixels area (step size squared) in log–log form (Clarke, 1986). The method derives a relationship between the surface area of triangular prisms defined by the grey-level values of the image and the step size of the grid used to measure the prism surface area.

(De Jong and Burrough, 1995) reported that TPM method underestimates the FD. An improvement, introduced by Qiu et al., 1999 allowed to the algorithm to correct this error.

Moreover the TPM was also found to be sensitive to noise or extreme grey-level values. However, beyond these limits, the method is the fastest and gives more accurate results than the BM and IM methods (Kolibal and Monde, 1998). The accuracy and efficiency of the three methods were evaluated on images from the Cantor set.

In 2006 Sun (2006) proposed three new methods to compute the fractal dimension based on Clarke's TPM method, called the max-difference method, the mean-difference method and the eight-pixel method. The proposed methods have been tested using both simulated fractal surfaces and real images. Results showed that the methods are more robust than the Clarke's method for synthetic images with complex textures.

5. Multifractal analysis

Multifractals could be seen as an extension of fractals. A multifractal object is more complex in the sense that it is always invariant by translation, although the dilatation factor needed to be able to distinguish the detail from the whole object depends on the detail being observed.

Multifractal analysis initially appeared with multiplicatives cascades models of Mandelbrot for the study of energy dissipation in the context of the fully developed turbulence then it was applied for the measurement of the turbulent flow velocity in the 1980s. In this latter situation, the velocity has a very complex structure; in particular, irregular behaviour occurs at "infrequent" places in the sense of a Lebesgue measurement in R^3. A signal treatment approach has been then developed which consisted to study the regularity of a signal with a velocity v. The aim is to define in each signal point x_0 the velocity variation law to deduce the punctual Hölder exponent $h(x_0)$.

Afterwards points with the same exponent h are grouped together into sets S_h. These sets might have a null Lebesgue measure. However if they are not significant in measure term, their topological dimension can be. Thus, physicists searched to compute the Hausdorff dimension D_h of S_h. The function $h \to D_h$ was called the singularity spectrum.

The direct determination by numerical computing of the singularity spectrum of a real signal proves to be difficult because the number of definitions to compute it is infinite. A formula, named "multifractal formalism" has been established by Parisi and Frisch in order to compute this spectrum. The multifractal formalism was then defined by:

$$D(h) = \inf_q (q \cdot h - \tau(q) + c) \tag{5}$$

where q is a real, c is a constant and $\tau(q)$ is called the partition function.

This formula is still difficult to apply for real signals, for this reason the topic of many works was the implementation of methods

to evaluate the generalized multifractal dimensions spectrum D_q, $q \in R$. The parameter q serves as a "microscope" for exploring different regions of the singular measurement. For $q > 1$, D_q represents the more singular regions, for $q < 1$, it accentuates the less singular regions and for $q = 1$, it represents the information dimension.

However, an alternative description can be formulated. Indeed, a multifractal structure can be considered as a superposition of homogeneous monofractal structures. Let us consider the set $E(h)$ of Hölder exponents h of particles with values in the interval $[h, h + \Delta h]$. $F(h)$ is defined as the FD of the set $E(h)$, which has a monofractal structure. The pairs $(q, \tau(q))$ and $(h, F(h))$ are linked by the Legendre transform:

$$\begin{aligned} \tau(q) &= q \cdot h(q) - F(h) \\ h(q) \cong \alpha(q) &= \frac{d\tau(q)}{dq} \end{aligned} \tag{6}$$

where α is an approximation of the Hölder coefficient h.

For a multifractal structure, the dimensions D_q are decreasing functions of q, and $h \to F(h)$ is a convex function whose maximum corresponds to the Hausdorff dimension D_h.

6. Multifractal spectrum computing methods

As for FD estimation, many methods exist to approximate the multifractal spectrum. We divided this description into two classes: first the methods said box-counting and the methods based on wavelets.

6.1. Box-counting methods

The methods of this class are based on the same principles than the methods for FD evaluation in Section 4.1. The signal is meshed with various boxes size r and a normalized measure is computed in each box.

6.1.1. Generalized fractal dimensions and multifractal spectrum

Standard box-counting techniques are used to analyse point's sets. Each set is described by an infinite number of generalized dimensions, D_q, also called "Renyi's dimensions" (Renyi, 1955), and by the multifractal spectrum $f(\alpha)$ (Halsey et al., 1986). The generalized dimensions D_q are computed as a function of the order of the probability moment q and then the multifractal spectrum can be obtained by Legendre transform.

The Legendre transform could lead to some errors (Veneziano et al., 1995). In 1989, Chhabra and Jensen defined a method for the direct estimation of the multifractal spectrum (Chhabra and Jensen, 1989). This method is widely used (Cuevas, 2003; Perrier et al., 2006; Wang et al., 2005).

These methods have the drawbacks of the box-counting methods but several computational refinements were reported (Block et al., 1990; Hou et al., 1990; Molteno, 1993).

Besides problems arising when the boxes contain few points, the algorithms are characterized by low statistics, emphasized by the negative exponents ($q < 0$); this, in turn, makes the measure to diverge exponentially (Feeny, 2000).

6.1.2. The "sand box" or cumulative mass method

The sandbox method, introduced by Tél et al. (1989) and developed by Vicsek (1990), is useful for the assessment of the generalized fractal dimensions for both positive and negative moment orders, q, permitting the reconstruction of the complete multifractal spectrum.

This method consists in randomly selecting N points belonging to the structure and then counting, for each point i, the number of pixels $M_i(r)$ that belong to the structure inside a disk of diameter r centred at this point. The generalized dimensions D_q are obtained using the mean of $M(r)$ for various r.

The advantage of this method is that the boxes are centred on the structure, so there are no boxes with too few elements (i.e. pixels) inside. Indeed, for $q < 0$, boxes that contain a small number of elements (because they barely overlap with the cluster) give anomalously large contributions.

The sandbox procedure represents a solution to the border effect problem (i.e. the presence of almost empty cells containing few points not centred in them), permitting the reconstruction of the multifractal spectrum also for negative q (De Bartolo et al., 2004).

Finally, we can quote that this method has just been developed for binarized signals.

6.1.3. The large-deviation multifractal spectrum

When the multifractal spectrum is estimated using the abovementioned methods, its shape is always concave. The advantage of the large-deviation multifractal spectrum is that it will not always be concave and so less information loss will occur. However, much more numerical computation is required and the method becomes difficult to apply in 2D and 3D. Indeed, the algorithm necessitates the calculation of two limits, instead of just one as for the two previous methods.

In view of the high computation cost, this method is primarily used for 1D signals (Broniatowski and Mignot, 2001; Touchette and Beck, 2005). This spectrum can also be applied to image segmentation (Abadi and Grandchamp, 2006).

6.2. Wavelet methods

The second class of methods are based on the wavelet transform. The wavelet transform of a signal is used like an "oscillating" box to represent its components. Therefore there is no need to mesh the signal.

Some methods use the discrete wavelet transform and others are based on the continuous wavelet transform.

6.2.1. Methods based on the discrete wavelet transform

The properties of multifractal formalism (based on discrete wavelet coefficients) were established by Jaffard (1997). This technique is founded upon result of Meyer (1998) showing that under mild regularity conditions on the paths of the process $x(t)$, the local Hölder exponent can be computed from size estimates of the wavelet coefficients $W_{j,k}$:

$$\alpha(t_0) = \lim_{k2^{-j} \to t_0} -\frac{1}{j}\log_2|W_{j,k}| \tag{7}$$

where $k2^{-j} \to t_0$ means that t_0 belongs to $[2^{-j}k, 2^{-j}(k+1)]$ as $j \to \infty$.

As with any working framework, multifractal formalism has a number of limitations. Firstly, q negative order exponents are meaningless. Indeed, there is no reason why discrete wavelet coefficients should be non-zero, and in practice they can have values very close to zero. Secondly, this formalism fails for signals which contain oscillating singularities (Meyer, 1998). Such oscillating singularities are shown to appear generically in local self-similar functions which are invariant under a nonhyperbolic mapping (Arneodo et al., 1995).

6.2.2. The wavelet transform modulus maxima (WTMM) method

This method is also based on the concept of wavelets in general and the use of the continuous wavelet transform in particular. It has been developed and used in one and two dimensions in several works (Bhatti et al., 2007; Enescu et al., 2006; Khalil et al., 2006;

Klapetek and Ohlidal, 2005). The method is more numerically stable than other methods for 1D and 2D dimensional multifractal spectrum calculation (such as the use of fractional Brownian motions, for example (Brodu, 2005). In (Kestener and Arneodo, 2003), the method was applied in 3D and the authors showed its robustness using simulated 3D multifractal models. The algorithm is based on the construction of wavelet transform modulus maxima chains.

The method presents some limits. It is more difficult to implement than the previous methods. It has some freedom degrees, like the wavelet choice and the scales number. However Kestener and Arneodo (2003) showed that it is more effective than the "box-counting" methods.

6.2.3. The wavelet leaders method

This method is a recent technique. It is based on the definition of wavelet leaders obtained by the discrete wavelet transform.

Although there is no study showing its effectiveness, it presents some benefits. Indeed, the estimated multifractal formalism has a mathematical validity and the right part of spectrum is valid ($q < 0$), meaning that the partition function (obtained by wavelet leaders) is also valid when $q < 0$. This formalism was theoretically proven by Jaffard et al. (2005) and then developed in 1D by Lashermes et al. (2005) for applications in fully developed turbulence.

7. Applications

Over the last years, fractal and multifractal analysis have been applied extensively in medical signals analysis. In this section, we classify and summarize these applications in many clinical procedures where 1D, 2D and 3D signals were involved.

Applications are grouped into the two main recurrent classes namely segmentation and characterization.

7.1. Segmentation

In many clinical applications, image segmentation is an important task which depends strongly on the signatures used to characterize a given region of the image. These signatures can be of several types; for example, one can characterize the pixels distribution heterogeneity of a region of the image. Multifractal models enable to describe the scale-to-scale propagation of this heterogeneity (Martinez et al., 1997).

Texture segmentation methods using the fractal and multifractal geometry can be divided into two classes:

- Methods based only on fractal and/or multifractal features.
- Methods that combine fractal and/or multifractal features with other texture features.

Fractal analysis can be used alone in texture segmentation. Keller et al. (1989) were the first to propose a method for texture segmentation using fractal geometry. Subsequently, a number of works (Hsu et al., 2007; Kikuchi et al., 2005; Zhuang and Meng, 2004) examined several fractal parameters.

Other methods were motivated by the use of some fractal geometry derived features, such as lacunarity and signatures (Dubuisson and Dubes, 1994). In fact, Espinal and Chandran (1998) demonstrated that a wavelet-based fractal signature was a very accurate and robust method for grey-scale texture classification and segmentation.

Kaplan (1999) introduced multiscale Hurst parameters for the characterization of various natural textures. The precision of this algorithm was notably assessed on mosaic texture images.

Ida and Sambonsugi (1998) applied fractal coding for image segmentation. The encoding method was the same as in the conventional fractal coding method. An image can be segmented by calculating bases on a dynamic system parameterized by fractal coding. The authors showed that the method was able to segment regions that have fine, clustered pixel patterns.

Lastly, the local FD was used with success to segment textures. The local FD is either computed for each pixel in the image or in local windows (Maeda et al., 1998). For instance, Novianto et al. (2003) presented an algorithm based on 3×3 windows.

In the second class of methods, fractal analysis is combined with other texture parameters like the Fourier spectrum, first and second-order statistics (the co-occurrence matrix), ... (Guo et al., 2007).

Lee et al. (2005) developed an unsupervised segmentation algorithm for ultrasonic liver images based on the multiresolution fractal feature vector.

One drawback of these methods is that they require classification (clustering); it is thus important to estimate the number of textures present in the image. In most cases, this estimation is difficult or even impossible to perform.

In some cases, fractal analysis does not perform correct image segmentation. Indeed, some images are complex to study because they present irregularities and more regular zones at all scales, without following a clear law. To recover information from such singular images, multifractal formalism suggests studying the way in which the image's singularities are distributed, i.e. the singularity spectrum, equivalent to the entropy. Thus, a number of recent studies have focused on texture segmentation using multifractal analysis (Abadi and Grandchamp, 2006; Xia et al., 2006) with application to MR and US images (Ezekiel, 2003).

Zhuang and Meng (2004) segmented ultrasound images using the local FD (Fig. 2). Lévy-Véhel et al. (1992) segmented MR images using a generalization of Chhabra's method and the results were conclusive (Fig. 3).

Xia et al. (2006) presented a novel multifractal estimation algorithm based on mathematical morphology and a set of new multifractal descriptors, namely the local morphological multifractal exponents. The latter are used to characterize the local scaling properties of the texture. Both the proposed algorithm and the box-counting based methods have been applied to the segmentation of texture mosaics and real images. Comparison of the results showed that morphological multifractal estimation can differentiate texture images more efficiently and provide more robust segmentations than do the box-counting based methods.

Brief summary: Image segmentation is a key step in many medical imaging based procedures. Many research groups worked to solve specific medical image segmentation problems, with good results (Duncan and Ayache, 2000; Pham et al., 1999); however, until now, the generalization of these systems to a wider range of applications has not been successful. For this reason, research groups still work on this application.

Fractal features are used, in this field, as additional texture parameters. Indeed, the FD showed interesting results in some image modalities like MR, CT and US. However, considered alone, it cannot provide a precise method of segmentation, since it is calculated on windows of the image.

In conclusion, the FD can be introduced as a feature in a classification algorithm. For example, it can add information in statistical-model-based algorithms.

From another side, multifractal analysis seems more adapted than the FD to the texture segmentation. Its advantage is to characterize the local scales properties in addition to the global properties. So it makes it possible to quantify the distribution of the local singularities (local morphological multifractal exponents).

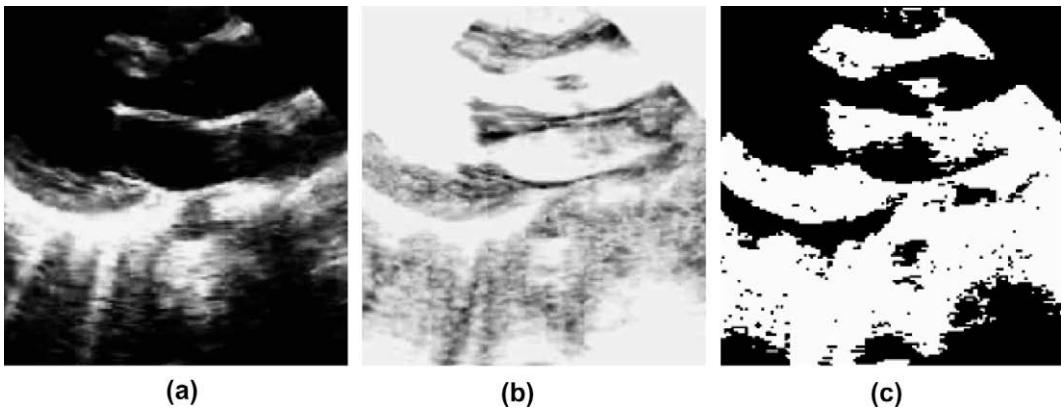

Fig. 2. Ultrasound image segmentation (a) the original image, (b) a local fractal dimension map and (c) the segmentation result (Zhuang and Meng, 2004).

Fig. 3. MR image of the eye and the corresponding segmentation (Lévy-Véhel et al. (1992)).

7.2. Characterization

Fractal and multifractal analyses have been used to study and to characterize a wide range of signals in biology and medicine (Kenkel and Walker, 1996; Landini and Rippin, 1996; Oczeretko et al., 2001). In this section, we limit our review to four main fields of application:

- electrocardiogram (ECG) and electroencephalogram (EEG) signals,
- brain imaging,
- mammography, and
- bone imaging.

In each field, applications in control group versus patient group characterization and abnormalities detection will be highlighted.

Before detailing the above applications, we discuss some other applications. Indeed, fractal geometry was used to characterize and quantify the response for cancer treatment (Imre and Bogaert, 2004; Jain et al., 2002; Wax et al., 2003). It was also used to describe spectral data used to study blood flow in the lungs (Glenny and Robertson, 1991), where the heterogeneity of pulmonary blood flow is not adequately described by gravitational forces alone. Krenz et al. (1992) used a fractal analysis to correlate the morphometric data from the intrapulmonary arteries with functional measurements of blood flow, in order to represent the haemodynamic consequences of the pulmonary arterial tree structure. The basis of myocardial flow heterogeneities (Bassingthwaighte et al., 1990) can be described by a natural fractal. There is also a fractal analysis of radiographs of the peridental alveolar bone (Ruttiman et al., 1992).

Spine neurons have been described in terms of FD. Keough et al. (1991) used fractal analysis to study electron micrographs of different cell types by using micrographs obtained at various magnifications and subsequently enlarged by different amounts. Cross et al. (1993) used a fractal analysis of renal angiograms to study the morphological complexity of the renal arterial tree and also (Cross et al., 1994) histological sections from molar and non-molar pregnancies and partial hydatidiform moles to determine whether the FD was discriminating between-groups.

Lastly, Stosic and Stosic (2006) showed that the vascular structures of human retina represented geometrical multifractals characterized by a hierarchy of exponents, rather than a single FD.

7.2.1. 1D EEG/ECG signals

Fractal analysis applied to medical signals is an active field of research. Indeed, some signals have a fractal character; this is particularly the case for repeated sequences, like palindromes (local repetitions) and homologies between two different nucleotide sequences (motifs along the genome) composing a self-similar (fractal) pattern in mitochondrial DNA (Oiwa and Glazier, 2004).

The FD has also been used to characterize two states or to predict a phenomenon. It is usually applied to ECG and EEG signals (Phothisonothai and Nakagawa, 2007; Smrcka et al., 2003) using the box-counting method.

To model an EEG, the signal is considered as a series of sine and cosine waves of constant amplitude (John and Bradford, 1993). In order to distinguish the classes of time series (EEG), which correlate to brain activities, fractal analysis is often used.

Fractal interpolation can also be used for ECG data compression (Jun et al., 1994).

FD can also be used as a method for discriminating between two states (Esteller et al., 2004; Li et al., 2005; Spasic et al., 2005).

Anderson et al. (1997) showed that the FD can be predictive for arrhythmic (but not non-arrhythmic) death in a large post-infarction cohort. Pereda et al. (1998) found in their study on human EEG (awake and sleep stages of the patient) that EEG exhibits random fractal structure with $1/f^{-\beta}$ spectrum, where the β exponent was between 1 and 3. More than the correlation dimension (D_2), β exponent is appropriate to correlate with the behaviour of EEG waves. Murali (2005) showed that FD was more sensitive than Fourier transform for applications in the prediction. Woyshville and Calabrese (1994) used fractal dimension in their studies on quantification of occipital EEG with respect to the Alzheimer disease for the three conditions defined as (1) controls, (2) probable Alzheimer disease and (3) autopsy-confirmed Alzheimer disease. They concluded that fractal dimensions clearly describe the EEG pathology and suggested that they have a potential clinical utility.

Recently, Hsu et al. (2007) presented a new electroencephalogram (EEG) analysis system using active segment selection and multiresolution fractal features (notably the differential box-counting method).

Multifractal algorithms have also been used (Li et al., 2005; Munoz et al., 2005; Xia et al., 2006; Yum and Kim, 2002). The principal application is discrimination between two states (Munoz et al., 2005; Wang et al., 2006). Wang et al. (2007) showed that the area value of the ventricular fibrillation singularity spectrum (VF) tended to be higher than the area value of the ventricular tachycardia singularity spectrum (VT), by using the direct determination method for the singularity spectrum $f(\alpha)$. This latter study is particularly interesting because it demonstrates the effectiveness of multifractal analysis comparing to other methods. Indeed, concerning VF and VT classification, several quantitative analysis techniques have been suggested, such as a sequential hypothesis testing algorithm (Thakor et al., 1990), a method based on complexity measurement (Zhang et al., 1999), a qualitative chaos analysis based on symbolic complexity (Zhang et al., 2002), the correlation dimension method (Small et al., 2002), the Lyapunov exponent method (Owis et al., 2002), and the entropy approximation method (Caswell Schuckers, 1998). However, none of these methods was able to distinguish VF from VT.

The generalized fractal dimensions have been used by Kulish et al. (2006) to show that these dimensions contain information related to both frequency and amplitude characteristics of the EEG signals.

Multifractal analysis can also be used to show the monofractal or multifractal nature of medical signals (Yum and Kim, 2002). In this case, the WTMM method is the most appropriate because it is the most numerically stable (Arneodo et al., 1998). The method provided good results with EEG signals (Popivanov et al., 2005; Shimizu et al., 2004).

Brief summary: The FD clearly has an advantage in the study of EEG signals, since these signals exhibited random fractal structure. As reported in this section, in a large number of applications (epilepsy, sleeping disorder, Alzheimer disease), FD showed its usefulness. Several methods for FD calculation are used and, even the methods with many limits like the "box-counting" methods, provided satisfactory results. Until now, there is no comparative study of the methods to highlight to most effective one for these signals. However, the FD clearly showed its advantage compared to other methods, like the Fourier transform. Recently, many reports on fractal dimension and fractal spectra analysis predicted the brain activities more precisely than Fourier transform. Even fractal spectra analysis has limitations in analysing stationary brain waves, multiple brain activities, ...

Multifractal analysis is also used successfully in various applications concerning the use of EEG signals. A numerically stable method (WTMM method) showed monofractal and multifractal characters of signals and provided good performances in the classification of two states. Thus, this method will continue to be an important area of research in study of EEG signals.

7.2.2. Brain imaging

Fractal dimension is the most frequently applied features in this field of application. One important early observation was that FD is not discriminative on MR brain images. Indeed, whole brain images from healthy subjects and patients have similar FD values (Cook et al., 1995; Free et al., 1996). In the first work, FD was computed using the box-counting method and in the second, it was computed for the contours of the brain using the morphological operator method. However, FDs were successfully used to quantify cells morphologies in the brain (Kalmanti and Maris, 2007; Smith et al., 1993; Smith and Behar, 1994; Soltys et al., 2001) and the brain shape (Blanton et al., 2001; Gorski and Skrzat, 2006; Iftekharuddin et al., 2000; Kedzia et al., 2002; Pereira et al., 2000; Rybaczuk et al., 1996; Thompson et al., 1996).

Some works were carried on the grey matter (GM) (Blanton et al., 2001; Liu et al., 2003; Sato et al., 1996; Sisodiya and Free, 1997), others focused on the white matter (Free et al., 1996; Liu et al., 2003; Shan et al., 2006).

Using MR images of the human brain, Bullmore et al. (1994) measured the boundary between the cerebral cortex and white matter, with application to the characterization of schizophrenics, manic-depressives and controls. The mean FD (computed by the box-counting method) was greater in boundaries extracted from manic-depressive patients than in those extracted from controls, whereas it was lower in schizophrenics than in controls. It was suggested that the FD is a useful measure of clinically relevant differences in the complexity of MRI boundaries.

Blanton et al. (2001) examined the influence of age and gender on the structural complexity and asymmetry of primary cortical sulci in normally developing children by computing the FD for the contour surface between the sulcus and the gyrus on brain MR images. The method was based on the algorithm presented by Thompson et al. (1996).

Kedzia et al. (2002) studied the microarchitecture of foetal brain blood vessels during pregnancy; they showed that the mean FD (computed by the box-counting method) was 1.26 during the fourth month, increased to 1.53 during the fifth month and then grew even more rapidly until the sixth and seventh months. This suggested an increased level of complexity and feed volume in the brain.

Liu et al. (2003) skeletonized the human cerebellum and showed that it has a highly fractal structure, with a FD (computed using the box-counting method) of 2.57. There were no significant differences between men and women in terms of the cerebellum FD.

Zhang et al., 2006 were the first to introduce a method to compute the 3D FD of three features of the human's brain: white matter, the interior structure, the surface (i.e. the interface between GM and WM) and the overall structure (the whole WM voxel set). The structural complexity of the WM declined with age in all anatomical structures analysed (whole brain and hemispheres). Age-related asymmetrical changes were found in the WM's interior structure: the complexity of the WM's interior structure decreased in the left hemisphere in men and in the right hemisphere in women. White matter structures in men were more complex (i.e. they had a higher FD) than in women. Lastly, an asymmetric complexity pattern (right side greater than left side) was observed for the WM interior and general structures, whereas the complexity of the WM surface was symmetrical. No significant age-related WM volume reductions were observed.

Fractal analysis has also been used for brain tumor detection (Iftekharuddin et al., 2003; Mansury and Deisboeck, 2004; Penn et al., 1999). Iftekharuddin et al. (2000) used the FD value to detect and locate brain tumors. The FD was computed using the fBf variance model method and used to extract information on tumor progression relative to normal brain data. Zook and Iftekharuddin (2005) presented an algorithm for brain tumor detection on 2D MR images. The principle was as follows: the FD of the left half of the brain was compared with that of the right half (assuming that the tumor is located in one half only). The authors found that the FD of tumor regions is usually lower than that of non-tumor regions. The authors also compared the efficiency of different methods of FD computation (piecewise modified box counting (PMBC) – piecewise triangular prism surface-area method (PTPSA) – blanket algorithm). Some of results are presented in Fig. 4. PMBC method detected the tumor inner as high FD in a 32×32 neighbourhood, while PMBC detected tumor edges as high FD in a 64×64 neighbourhood (Fig. 4b and c). For the same image, PTPSA detected the tumor as slightly higher FD and blanket algorithm detected part of the tumor as higher FD (Fig. 4d and e). Specifically, in this study, the PTPSA algorithm was more predictive at lower resolutions and the blanket algorithm was more predictive at higher resolutions. Furthermore, in a 8×8 neighbourhood, the PTPSA algorithm offered the best tumor detection performance.

Moreover, results concerning the 3D fractal analysis used in brain single photon emission computed tomography (SPECT) for the characterization of Alzheimer's disease were presented (Nagao and Murase, 2002; Takahashi et al., 2006; Yoshikawa et al., 2003). The FD is estimated by a method which lacks a true theoretical basis, a generalization of the box-counting method. Indeed, this method was refuted by (Chung, 2003) because the FDs obtained were between 1 and 2, whereas they should be between 3 and 4. In another study, (Lopes et al., 2007a) used a 3D adaptation of the differential box-counting method to derive the 3D FD and applied it for the characterization of epilepsy in SPECT imaging.

There are fewer published works on multifractal analysis. Takahashi et al. (2006) used the Chhabra spectrum to quantitatively evaluate white matter hyperintensity. Lopes et al. (2008) used a 3D adaptation of Chhabra's method to characterize the local changes in homogeneity in brain SPECT images. There was a statistically significant difference between the control group and the pathological group.

Brief summary: The studies are mainly done on brain magnetic resonance imaging (MRI). The use of FD on the brain MRI required a special attention, since two studies showed that the FD did not make it possible statistically to separate the healthy subjects and the patients. However this remark can be discussed, for example the first study used the box-counting method, therefore there was a binarization in pre-processing and this step could remove important information. Then there have been only a few fractal studies on non-linear structures observed by brain magnetic resonance imaging, and the contents of these studies have been mostly limited to extraction of fractal structures (white matter surface, cortical/subcortical boundary). However the FD proved to be a discriminating tool for some structures.

The FD has also been used for brain tumor detection with limited results. Indeed the information brought by the FD was interesting, but it would be necessary to add other information for a better segmentation. Thus, the FD can be used like an additional feature in segmentation algorithms.

Finally first works concerning the use of the multifractal analysis were interesting, but they used "box-counting" methods, it will be interesting to see the influence of a wavelet-based method.

7.2.3. Bone trabeculation

It was already well known that both trabecular bone density and structure affect overall bone quality and strength (Cooper, 1993; Dempster et al., 1993; Ott, 1986; Uitewaal et al., 1987). Indeed in biomechanical terms, fracture risk for an osteoporotic is determined by the combination of factors inherent to the bone quality (e.g. cortical thickness, mineral contents, trabecular bone density and microarchitecture). One of the most important factors contributing to bone strength is its complex structure. Bone has two components: an outer part consisting of a tube of very dense material and an inside that looks like a sea sponge, filled with finely interlaced struts, called trabeculae, which are about as wide as a human hair.

The first computerized analysis for trabecular architecture quantification was done by the use of morphological measures. These measures showed moderate to good relationship with Bone Mineral Density (BMD) (Link et al., 1997; Ouyang et al., 1998), but not many of the measures significantly complement BMD to the prediction of biomechanical properties. The idea has also been to use measures of second-order statistics, especially the fractal analysis. Many studies were done to validate the use of fractal analysis in this application. The early studies were concerned with establishing methodology or determining if cancellous bone is indeed fractal in nature. One of the properties of theoretical fractal shapes is that they have an indeterminate perimeter. Cancellous bone has been showed to have this property (Parkinson and Fazzalari, 1994). Specially, if the perimeter and area of a histological section of cancellous bone is measured at increasingly higher magnification, the measured perimeter will increase but the measured area will remain relatively constant. A second property of the fractal geometry is the self-similarity (in the statistically sense) of objects. Benhamou et al. (1994) proved the self-similarity of the trabecular bone microarchitecture on calcaneus radiographs.

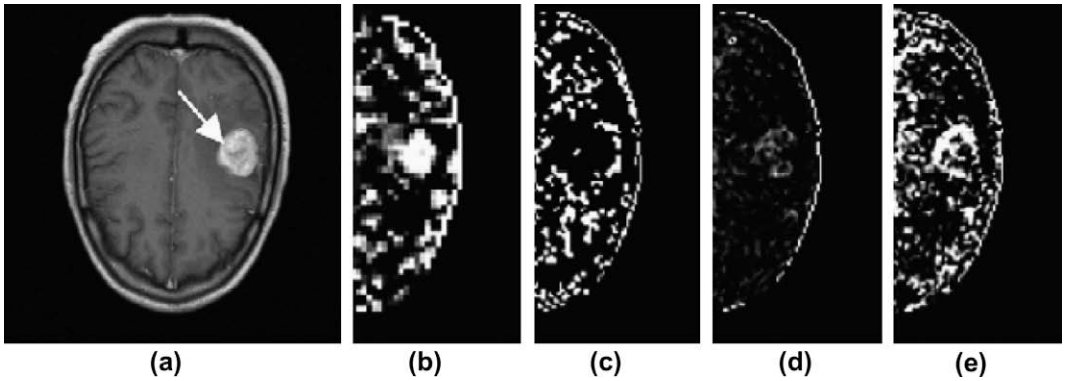

Fig. 4. (a) A T1 MR image with contrast agent. Also shown are positive FD difference results for (b) PMBC-32, (c) PMBC-64, (d) PTPSA and (e) the blanket method (Zook and Iftekharuddin, 2005).

Many studies were done by comparing control group and patients group to show that the FD is a discriminative measure. Caligiuri et al. (1994) presented an analysis of lumbar spine radiographs. The authors used a surface-area technique to calculate the fractal dimension of radiographs, and have shown what appears to be a promising discrimination between subjects with and subjects without fractures. Khosrovi et al. (1994) showed differences between normal and osteoporotic women using fractal measures derived from wrist radiographs. Benhamou et al. (1994) showed that fractal measures derived from calcaneus radiographs may also be potentially useful in studying osteoporotic populations.

In 1999, a study by Majumdar et al. (1999) showed others important characteristics using fractal analysis in this application. They used three methods to compute the FD: a surface-area technique, a semi-variance technique and a Fourier transform technique. As it was stressed in Section 4, many methods exist to evaluate the FD, but with different results. The authors used three methods and their first result was that there was a correlation between the fractal dimensions of the three methods and the micro-architectural measures of trabecular structure. The second result was that the semi-variance and Fourier transform techniques showed differences between the trabecular orientation in the vertebrae and the other planes, while the surface-area technique did not discriminate between the planes. This result can be explained by the fact that the semi-variance and Fourier transform techniques are based on a stochastic formulation, while the surface-area technique is based on a deterministic theory. Thus, the similarity between the semi-variance and the Fourier transform results and the discrepancy between the surface-area based results is not unexpected. The important message in this paper was that different fractal techniques provided different results. These measures can adequately be exploited to provide different kinds of information pertaining to bone strength and structure.

In the recent years, research on bone trabeculation through fractal analysis has remained very dynamic (Messent et al., 2005; Papaloucas et al., 2005; Wilkie et al., 2004; Yasar and Akgunlu, 2006). Many studies concerned bone trabeculation anisotropy. Yi et al. (2007) measured bone trabeculation anisotropy using directional FDs (calculated as a function of orientation and which yielded the fractal information reflecting the spatial characteristics of the trabecular bone in each direction). They found that the anisotropy was significantly higher in the angle region of the mandible than in the incisor region. (Jennane et al., 2006) estimated the anisotropy degree of fractal on bone X-ray images, known to be complex in terms of their non-stationarity, anisotropy and textured character. They demonstrated that the bone organization was more anisotropic for osteoporotic subjects than for healthy controls, in accordance with the natural osteoporosis-related changes in bone tissue. The authors computed the FD using the variogram method. Later on, it will be shown that the use of this method presents the following limitation: more the structure is complex, more the FD increases. However the method is unstable for surfaces of higher dimensions (Lam et al., 2002).

Finally and always in the healthy control/patient classification applications, Taleb-Ahmed et al. (2003) suggested a way to characterize bone texture in CT images, with a view to discriminating between healthy and pathological subjects. In other studies (Dougherty, 2001; Dougherty and Henebry, 2001), lacunarity parameters were combined with the fractal signature to improve the healthy control/patient classification.

Brief summary: During the past decades, there has been continuous investigation into the use of fractal analysis in bone trabeculation applications. Several applications have been studied as the fractal character of the trabecular bone. This property, revealed in 1994 by Benhamou et al., made it possible to validate the use of FD in these applications. From this, many studies have been carried out, in particular the comparison between normal subjects and diseased subjects, bone trabeculation anisotropy, etc.

Concerning the FD computing algorithms used, studies showed that some methods allowed good performances whereas others did not bring any information. This point confirms the previous assertion, namely that the methods provide different results and showed the importance of the method's choice. In the applications concerning the trabecular bone, the Fourier transform based method seemed to provide of the most stable results.

Finally there are not real applications of the multifractal analysis for trabecular bone studies, which can be explained by the fact that encouraging results have been obtained with FD. As we mention it above, multifractal analysis adds local information about the signal heterogeneity. In these applications, this information was not fundamental, but just a global quantification of the signal was necessary.

7.2.4. Mammography

Mammography is the principal tool for the detection and diagnosis of breast cancer. Clinical studies demonstrated that survival is greatly improved if the breast anomalies are detected at early stages (Tabar et al., 1993). One of the significant signs of possible cancerous changes is the existence of small mineral deposits in the breast tissue, usually referred as micro-calcifications (Suri et al., 2002). Currently, mammography is the most effective tool for detecting possible breast anomalies, including micro-calcifications. It consists of an X-ray radiographic examination of each breast, usually from two angles (a top-to-bottom view and an oblique view). Others imaging modalities (ultrasound, MR) can be used but only as complementary examinations in the event of a difficult diagnosis. However, micro-calcifications with small sizes (typically up to a few of millimeters) and low contrast are difficult to detect. Thus, by applying image processing algorithms, significant improvements for the detection of micro-calcifications were possible.

In particular, the application of fractal geometry showed interesting results. There are many reports on the use of this geometry in mammography images (Li et al., 2007; Nguyen and Rangayyan, 2005; Tanki et al., 2006).

In this field, the applicability of the fractal geometry is justified by the fact that, micro-calcifications usually appear as a cluster of bright spots with variant size and shape embedded in an inhomogeneous background of breast tissue. The inhomogeneous background also exhibits the self-similarity property of typical fractal images such that a region of interest in digital mammograms containing the micro-calcifications clusters can be viewed as a fractal normal background superimposed by a non-fractal foreground (i.e. the micro-calcifications clusters) (Huang and Yu, 2007; Kestener et al., 2004).

For breast density measurements, Caldwell et al. (1990), Taylor et al. (1994) and Byng et al. (1996) used various fractal indices to classify the images into categories. In particular, Byng et al. (1996) used a 3D box-counting method to calculate the surface FD (x, y, $I(x, y)$) where $I(x, y)$ is the grey-scale value at pixel (x, y). The FD is estimated for the totality of the breast. The obtained FD values are ranged between 2.23 (for a dense breast) and 2.54 (for a fatty breast), corresponding to Hurst exponent values of 0.77 and 0.46, respectively.

Kestener et al. (2004) showed that the multifractal spectrum computed by the WTMM method allows discrimination between fat and dense tissues. The authors found that dense and fat tissues had Hurst exponent values of 0.65 and 0.3, respectively. This approach reached to similar results as those provided by Byng et al., but the method used by Kestener et al. was more robust. Indeed, Byng et al. used the box-counting method while Kestener et al. used the WTMM method. Moreover the second study showed

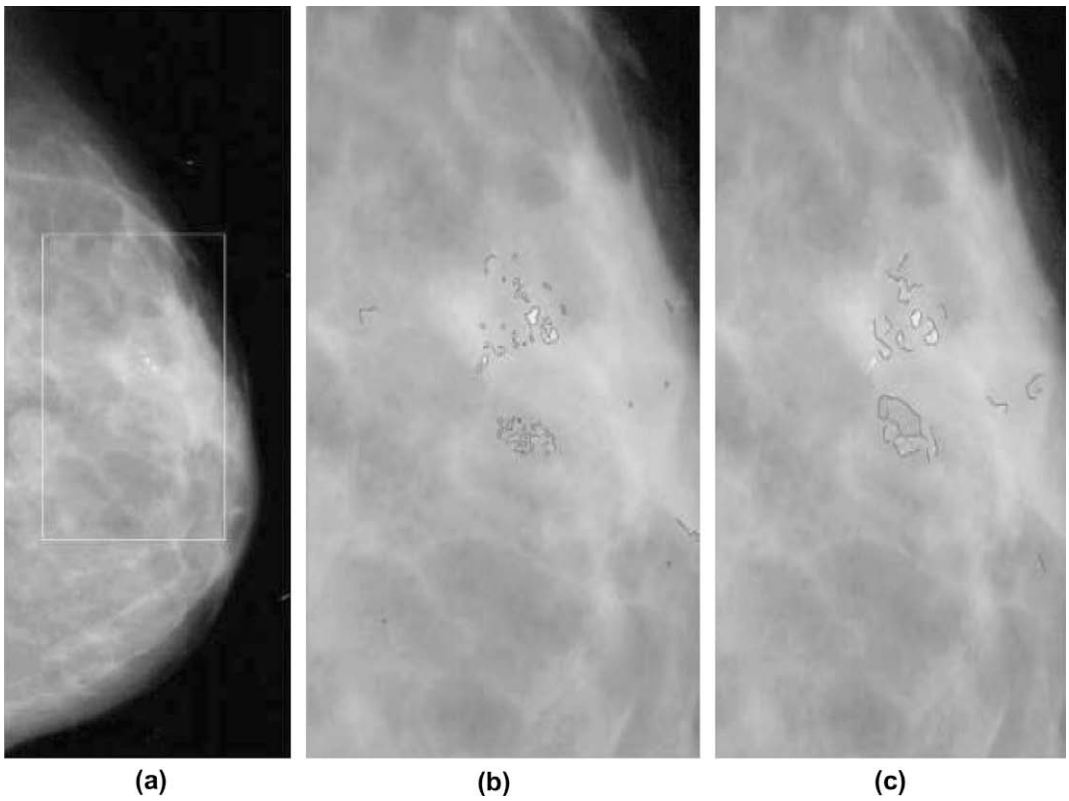

Fig. 5. Micro-calcification detection in a mammography containing two malignant foci. (a) The original mammography: the white rectangle indicates the region of interest. (b) and (c) show the maxima chains resulting from the maxima lines sorting procedure indicating the micro-calcifications for scaling parameter values of $a = 1$ and $a = 4$, respectively (Kestener et al., 2004).

that the breast texture on mammography had not multifractal character.

Another application of fractal analysis concerned the enhancement of micro-calcifications on mammograms was that of Li et al. (1996). The authors showed that general mammographic parenchymal and ductal patterns can be well modelled by the fractal geometry. Therefore, micro-calcifications could be enhanced by taking the difference between the original mammogram and the modelled one. Their results were compared with those of the partial wavelet reconstruction and morphological operation approaches. The result demonstrated that the fractal modelling method is an effective way to enhance micro-calcifications and thereby facilitates the radiologist's diagnosis.

Fractal and multifractal analysis have also been used for benign/malignant classification and micro-calcification detection. These analyses were based on a number of features selected by radiologists (Lanyi, 1986; Veldkamp et al., 2000). Based on these features, Mavroforakis et al. (2006) used the FD (calculated by the box-counting method) as a texture characteristic for classification. The results showed a breast micro-calcification detection rate of about 83.9%. Rangayyan and Nguyen (2005) showed that FD computation (using the grid method) for micro-calcification contours enables classification of benign and malignant clusters. They also showed the efficiency of FD relative to other shape factor methods (compactness, the spiculation index, fractional concavity, Fourier factor).

The study by Guillemet (1996) constituted an initial approach to the application of multifractal analysis to micro-calcification detection. The proposed multifractal algorithm was based on the classic multifractal formalism for measurements (Lévy-Véhel, 1995; Lévy-Véhel and Vojak, 1995) and their numerical implementation used Chhabra's method (Chhabra and Jensen, 1989). The key point of this work consisted in finding a measurement deduced from a micro-calcification-containing image and then applying multifractal analysis to it in order to reveal the presence of micro-calcifications.

Using the generalized dimension spectrum D_q (Badii and Politi, 1984, 1985; Grassberger et al., 1988; Grassberger and Procaccia, 1983) as a discriminating factor, a non-supervised classification study showed a degree of specificity for the generalized dimensions method in the presence of micro-calcifications.

In 2004, a work by Kestener et al. (2004) reported good results for micro-calcification classification. The authors used the 2D WTMM method for texture classification in mammography via Hurst exponent calculation. They performed dense/fatty segmentation. Moreover, using the wavelet transform skeleton, they located and characterized micro-calcifications (Arneodo et al., 2003; Kestener et al., 2004) (Fig. 5).

More recently, (Stojic et al., 2006) used local multifractal analysis (and Chhabra's method in particular) to detect micro-calcifications. However this method was dependent on the micro-calcifications size. Moreover the authors used a "box-counting" method to compute the $f(\alpha)$ spectrum, which presents some drawbacks.

Brief summary: Fractal geometry has been intensively used in mammography for the diagnosis of breast cancer. FD has been used in studies of benign/malignant classifications and detection of micro-calcifications. With regard to the first application the FD could be a discriminating tool, but it was really effective when it was combined with other texture features. For the second application, the FD is able to isolate micro-calcifications areas but it is not able to segment them precisely. Precisely in this second application multifractal analysis could be an interesting tool. Indeed the

Table 1
The main fractal and multifractal methods and medical image applications.

Methods	Applications					
	Segmentation	Characterization				Others
		EEG/ECG signals	Brain images	Bone texture	Mammography	
Fractal						
Box counting	Keller et al. (1989)	Anderson et al. (1997), Smrcka et al. (2003) and Phothisonothai and Nakagawa (2007)	Smith et al. (1993), Smith and Behar (1994), Bullmore et al. (1994), Cook et al. (1995), Soltys et al. (2001), Kedzia et al. (2002), Liu et al. (2003), Zhang et al. (2006), Gorski and Skrzat (2006) and Kalmanti and Maris (2007)	Majumdar et al. (1999), Wilkie et al. (2004) and Yasar and Akgunlu (2006)	Byng et al. (1996), Nguyen and Rangayyan (2005), Mavroforakis et al. (2006), Tanki et al. (2006) and Li et al. (2007)	
Differential box counting	Chaudhuri and Sarkar (1995)	Yum and Kim (2002)	Zook and Iftekharuddin (2005) and Lopes et al. (2007a)			
Extended counting method						Sandau and Kurz (1997) and Chung et al. (2002)
Triangular prisms method			Zook and Iftekharuddin (2005)			Oczeretko et al. (2001) and Imre and Bogaert (2004)
Covering blanket method	Novianto et al. (2003)		Zook and Iftekharuddin (2005)			
Variogram			Iftekharuddin et al. (2000)	Benhamou et al. (1994) and Jennane et al. (2006)		
Power spectrum				Caldwell et al. (1998), Ouyang et al. (1998), Lespessailles et al. (1998) and Majumdar et al. (1999)		
Isarithm method			Free et al. (1996)		Rangayyan and Nguyen (2005)	
Multifractal						
Renyi's dimensions	Xia et al. (2006)	Yu et al. (2001)			Guillemet (1996)	
Direct determination method of the f(α) singularity spectrum	Lévy-Véhel et al. (1992)	Wang et al. (2006) and Wang et al. (2007)	Takahashi et al. (2006) and Lopes et al. (2007b)		Stojic et al. (2006)	
Sand box method			Stosic and Stosic (2006)			
Large-deviation multif. Spect.						
Discrete wavelet transform		Li et al. (2005) and Hsu et al. (2007)				
The WTMM method		Arneodo et al. (1998), Shimizu et al. (2004) and Popivanov et al. (2005)			Kestener et al. (2004)	
Wavelet leaders						

WTMM method is efficient in the detection of the micro-calcifications.

8. Conclusion

Fractal geometry provides a powerful tool for the characterization and segmentation in many medical imaging applications. The applicability of this geometry in image analysis comes from the fact that the imaged object are discontinuous, complex, and fragmented. The significance and the advantage of this geometry compared to classic signal processing methods, lie in the way of how the non-regularities are assumed.

Fractal analysis is often brought to the evaluation of the FD which allows having a global description of the inhomogeneities in the image. Its efficiency has been demonstrated in classification and segmentation experiments where it was used as an additional texture parameter. It has also been used alone for the characterization of two states (e.g. healthy vs. pathological). Table 1 summarizes the main methods and applications used in the medical field. From this table, it appears that the box-counting method is the most widely used, despite its drawbacks (binarization of the signal, construction of empty boxes, grid effect, etc.). This generalization is easily understood because this method is easy to implement. Another explanation for the lack of interest in some methods among biomedical researchers is that these methods were developed outside the biomedical domain.

Beyond its advantage, the multiplication of computation methods of FD does not go without drawbacks. Indeed, the computed dimension could be affected by some parameters as the computation algorithm used and its parameters tuning. As result, it is difficult to know whether the observed differences in computed FD values is a result of true differences in image texture or a result

of certain arbitrary decisions made during the estimation process. Therefore, the choice of a method is an important issue in the computation of FD. In most applications cited in this study, no comparative evaluation was done to determine the most suitable algorithm for the considered data, which suggests that some results could be improved.

Another limitation with fractal analysis is to describe objects by a single fractal value whereas they exhibit a multifractal behaviour. Multifractal analysis is a response to this limit. It allows computing a spectrum or a set of fractal dimensions. However, as above, many algorithms exist to evaluate this spectrum and numerical differences between the methods appear.

As conclusion of this study, fractal geometry could be an efficient tool to deal with some problems in image analysis as long as two parameters are taken into consideration:

1. The dimensionality of images to choose fractal or multifractal analysis.
2. The suitable algorithm: To make a comparative study of the behaviour of the different methods on the data.

References

Abadi, M., Grandchamp, E., 2006. Texture features and segmentation based on multifractal approach. The 11th Iberoamerican Congress on Pattern Recognition 4225, 297–305.

Anderson, J., Karagounis, L., Stein, K., Moreno, F., Ledingham, R., Hallstrom, A., 1997. Predictive value for future arrhythmic events of fractal dimension, a measure of time clustering of ventricular premature complexes, after myocardial infarction. Journal American College of Cardiology 30 (1), 226–232.

Appleby, S., 1996. Multifractal characterization of the distribution pattern of the human population. Geographical Analysis 28 (2), 147–160.

Arneodo, A., Bacry, E., Muzy, J., 1995. Oscillating singularities in locally self-similar functions. Physical review Letters 74 (24), 4823–4826.

Arneodo, A., Decoster, N., Kestener, P., Roux, S., 2003. A wavelet-based method for multifractal image analysis : from theoretical concepts to experimental applications. In: Advances in Imaging and Electron Physics, P.W. Hawkes, Academic Press (Eds), Vol. 126, 1–98.

Arneodo, A., Bacry, E., Jaffard, S., Muzzy, J., 1998. Singularity spectrum of multifractal functions involving oscillating singularities. Journal of Fourier Analysis and Applications 4 (2), 159–174.

Asvestas, P., Matsopoloulos, G., Nikita, K., 1998. A power differentiation method of fractal dimension estimation for 2-D signals. Journal of Visual Communication and Image Representation 9 (4), 392–400.

Bachelier, L., 1900. Théorie de la spéculation. Annales scientifiques de l'École Normale Supérieure 17 (3), 21–86.

Badii, R., Politi, A., 1984. Hausdorff dimension and uniformity factor of strange attractors. Physical Review Letter 52 (19), 1661–1664.

Badii, R., Politi, A., 1985. Statistical description of chaotic attractors: the dimension function. Journal of Statistical Physics 40 (5–6), 725–750.

Bassingthwaighte, J., Van Beek, J., King, R., 1990. Fractal branchings: The basis of myocardial flow heterogeneities? Annals of the New York Academy of Science 591 (1), 392–401.

Benhamou, C., Lespesailles, E., Jacquet, G., Harba, R., Jennane, R., Loussot, T., Tourliere, D., Ohley, W., 1994. Fractal organization of trabecular bone images on calcaneus radiographs. Journal of Bone and Mineral Research 9 (12), 1909–1918.

Bhatti, A., Nahavandi, S., Frayman, Y., 2007. 3D depth estimation for visual inspection using wavelet transform modulus maxima. Computers and Electrical Engineering 33 (1), 48–57.

Bisoi, A., Mishra, J., 2001. On calculation of fractal dimension of images. Pattern Recognition Letters 22 (6–7), 631–637.

Biswas, M., Ghose, T., Guha, S., Biswas, P., 1998. Fractal dimension estimation for texture images: A parallel approach. Pattern Recognition Letters 19 (3–4), 309–313.

Blanton, R., Levitt, J., Thompson, P., Narr, K., Capetillo-Cunliffe, L., Nobel, A., Singerman, J., 2001. Mapping cortical asymmetry and complexity patterns in normal children. Psychiatry Research 107 (1), 29–43.

Block, A., Bloh, W., von Schellnhuber, H., 1990. Efficient boxcounting determination of generalized fractal dimensions. Physical Review A 42 (4), 1869–1874.

Brodu, N., 2005. Multifractal Feature Vectors for Brain-Computer Interfaces. Proceedings of the IEEE World Congress on Computational Intelligence 2883, 2890.

Broniatowski, M., Mignot, P., 2001. A self-adaptive technique for the estimation of the multifractal spectrum. Statistics and Probability Letters 54 (2), 125–135.

Bullmore, E., Brammer, M., Harvey, I., Persaud, R., Murray, R., Ron, M., 1994. Fractal analysis of the boundary between white matter and cerebral cortex in magnetic resonance images: A controlled study of schizophrenic and manic-depressive patients. Psychological Medicine 24 (3), 771–781.

Byng, J., Boyd, N., Fishell, E., Jong, R., Yaffe, M., 1996. Automated analysis of mammographic densities. Physics in Medicine and Biology 41 (5), 909–923.

Caldwell, C., Stapleton, S., Holdsworth, D., Jong, R., Weiser, W., Cooke, G., Yaffe, M., 1990. Characterization of mammographic parenchyma pattern by fractal dimension. Physics in Medicine and Biology 35 (2), 235–247.

Caldwell, C., Moran, E., Bogoch, E., 1998. Fractal dimension as a measure of altered trabecular bone in experimental inflammatory arthritis. Journal of Bone and Mineral Research 13 (6), 978–985.

Caligiuri, P., Giger, M., Favus, M., 1994. Multifractal radiographic analysis of osteoporosis. Medical Physics 21 (4), 503–508.

Caswell Schuckers, S., 1998. Approximate entropy as a measure of morphologic variability for ventricular tachycardia and fibrillation. Computers in Cardiology 1998 (13–16), 265–268.

Chappard, D., Chennebault, A., Moreau, M., Legrand, E., Audran, M., Basle, M.F., 2001. Texture analysis of X-ray radiographs is a more reliable descriptor of bone loss than mineral content in a rat model of localized disuse induced by the clostridium botulinum toxin. Bone 28 (1), 72–79.

Chaudhuri, B., Sarkar, N., 1995. Texture Segmentation Using Fractal Dimension. IEEE Transactions on Pattern Analysis and Machine Intelligence 17 (1), 72–77.

Chen, S., Keller, J., Crownover, R., 1993. On the calculation of fractal features from images. IEEE Transactions on Pattern Analysis and Machine Intelligence 15 (10), 1087–1090.

Chhabra, A., Jensen, R., 1989. Direct determination of the f(alpha) singularity spectrum. Physical Review Letter 62 (12), 1327–1330.

Chung, H., 2003. Fractal Analysis of Nuclear medicine Images Again: Validity and Interpretation of Results from New Analysis Methods. The Journal of Nuclear Medicine 44 (2), 316–317.

Chung, H., Wu, W., Chung, H., 2002. A reinvestigation of the extended counting method for fractal analysis of the pial vasculature. Journal of Cerebral Blood Flow & Metabolism 22 (3), 361–363.

Clarke, K., 1986. Computation of the fractal dimension of topographic surfaces using the triangular prism surface area method. Computers & Geosciences 12 (5), 713–722.

Cook, M., Free, S., Manford, M., Fish, D., Shorvon, S., Stevens, J., 1995. Fractal description of cerebral cortical patterns in frontal lobe epilepsy. European Neurology 35 (6), 327–335.

Cooper, C., 1993. The epidemiology of fragility fractures: is there a role for bone quality? Calcified Tissue International 53 (Suppl. 1), 23–26.

Cross, S., Howat, A., Stephenson, T., Cotton, D., Underwood, J., 1994. Fractal geometric analysis of material from molar and non-molar pregnancies. Journal of Pathology 173 (2), 115–118.

Cross, S., Start, R., Silcocks, P., Bull, A., Cotton, D., Underwood, J., 1993. Quantitation of the renal arterial tree by fractal analysis. Journal of Pathology 170 (4), 479–484.

Cuevas, E., 2003. F(alpha) multifractal spectrum at strong and weak disorder. Physical Review B 68, 24206–24212.

De Bartolo, S., Gaudio, R., Gabriele, S., 2004. Multifractal analysis of river networks: sandbox approach. Water Resources Research 40 (2), W02201.

De Jong, S.M., Burrough, P.A., 1995. A fractal approach to the classification of Mediterranean vegetation types in remotely sensed images. Photogrammetric Engineering & Remote Sensing 61 (8), 1041–1053.

Dempster, D., Ferguson, P., Mellish, R., Cochran, G., Xie, F., Fey, C., Horbert, W., Parisien, M., Lindsay, R., 1993. Relationships between bone structure in the iliac crest and bone structure and strength in the lumpar spine. Osteoporosis International 3, 90–96.

Dougherty, G., 2001. A comparison of the texture of computed tomography and projection radiography images of vertebral trabecular bone using fractal signature and lacunarity. Medical Engineering and Physics 23 (9), 313–321.

Dougherty, G., Henebry, G., 2001. Fractal signature and lacunarity in the measurement of the texture of trabecular bone in clinical CT images. Medical Engineering and Physics 23 (6), 369–380.

Dubuisson, M., Dubes, R., 1994. Efficacy of fractal features in segmenting images of natural textures. Pattern Recognition Letters 15 (4), 419–431.

Duncan, J., Ayache, N., 2000. Medical image analysis: progress over two decades and the challenges ahead. IEEE Transactions on Pattern Analysis and Machine Intelligence 22 (1), 85–105.

Enescu, B., Ito, K., Struzik, Z., 2006. Wavelet-based multiscale resolution analysis of real and simulated time-series of earthquakes. Geophysical Journal International 164 (1), 63–74.

Espinal, F., Chandran, R., 1998. Wavelet-based fractal signature for texture classification. Proc. SPIE of Wavelet Applications V 3391, 602–611.

Esteller, R., Echauz, J., Tcheng, T., 2004. Comparison of line length feature before and after brain electrical stimulation in epileptic patients. Proceedings of the 26th Annual International Conference of the IEEE Engineering in Medicine and Biology Society 7, 4710-4713.

Ezekiel, S., 2003. Medical Image Segmentation using multifractal analysis. Proceedings of the Applied Informatics 378, 220–224.

Feeny, B., 2000. Fast multifractal analysis by recursive box covering. International Journal of Bifurcation and Chaos 10 (9), 2277–2287.

Free, S., Sisodiya, S., Cook, M., Fish, D., Shorvon, S., 1996. Three-dimensional fractal analysis of the white matter surface from magnetic resonance images of the human brain. Cerebral Cortex 6 (6), 830–836.

Frish, U., 1995. Turbulence: the Legacy of A.N Kolmogorov. Cambridge University Press (Eds), Cambridge (UK), 296 pp.

Glenny, R., Robertson, H., 1991. Fractal modeling of pulmonary blood flow heterogeneity. Journal of Applied Physiology 70 (3), 1024–1030.

Goodchild, M., 1980. Fractals and the accuracy of geographical measures. Mathematical Geology 12 (2), 85–98.
Gorski, A.Z., Skrzat, J., 2006. Error estimation of the fractal dimension measurements of cranial sutures. Journal of Anatomy 208 (3), 353–359.
Grassberger, P., Badii, R., Politi, A., 1988. Scaling laws for invariant measures on hyperbolic and nonhyperbolic atractors. Journal of Statistical Physics 51 (1–2), 135–178.
Grassberger, P., Procaccia, I., 1983. Characterization of strange attractors. Physical Review Letter 50 (5), 346–349.
Guillemet, H. Détection et caractérisation des foyers de micro calcifications en mammographie numérique. 1996. Ecole Nationale Supérieure des Télécommunications, Paris, France, 171 pp.
Guo, Q., Shao, J., Guo, F., Ruiz, V., 2007. Classification of mammographic masses using geometric symmetry and fractal analysis. International Journal of Computer Assisted Radiology and Surgery 2 (Suppl. 1), 336–338.
Halsey, T., Jensen, M., Kadanoff, L., Procaccia, I., Shraiman, B.I., 1986. Fractal measures and their singularities: the characterization of strange sets. Physical Review A 33 (2), 1141–1151.
Haralick, R., Shanmugan, K., Dinstein, I., 1973. Textural features for image classification. IEEE Transactions on Systems, Man and Cybernetics 3, 610–621.
Hou, X., Gilmore, R., Mindlin, G., Solari, H., 1990. An efficient algorithm for fast O(N∗ln(N)) box-counting. Physics Letters A 151 (1–2), 43–46.
Hsu, W.Y., Lin, C.C., Ju, M.S., Sun, Y.N., 2007. Wavelet-based fractal features with active segment selection: application to single-trial EEG data. Journal of Neuroscience Methods 163, 145–160.
Huang, Y., Yu, S., 2007. Recognition of micro-calcifications in digital mammograms based on Markov random fiels and deterministic fractal modeling. Proceedings of the 29th Annual International Conference of the IEEE Engineering in Medicine and Biology Society, 3922-3925.
Ida, T., Sambonsugi, Y., 1998. Image segmentation and contour detection using fractal coding. IEEE transactions on circuits and systems for video technology 8 (8), 968–975.
Iftekharuddin, K., Jia, W., Marsh, R., 2000. A fractal analysis approach to identification of tumor in brain MR images. Proceedings of the 22nd Annual International Conference of the IEEE Engineering in Medicine and Biology Society 4, 3064-3066.
Iftekharuddin, K., Jia, W., Marsh, R., 2003. A fractal analysis of tumor in brain MR images. Machine Vision and Applications 13 (5), 352–362.
Imre, A.R., Bogaert, J., 2004. The fractal dimension as a measure of the quality of habitats. Acta Biotheoretica 52 (1), 41–56.
Jaffard, S., Abry, P., Lashermes, B., 2005. Wavelet leaders in multifractal analysis. In: Wavelet analysis and Applications, T. Qian, M.I. Vai, X. Yuesheng, Birkhäuser Verlag (Eds), 219–264.
Jaffard, S., 1997. Multifractal formalism for functions. SIAM Journal of Mathematical Analysis 28, 944–970.
Jain, R., Munn, L., Fukumura, D., 2002. Dissecting tumour pathopsysiology using intravital microscopy. Nature Reviews Cancer 2 (4), 266–276.
Jennane, R., Harba, R., Lemineur, G., Bretteil, S., Estrade, A., Benhamou, J., 2006. Estimation of the 3D self-similarity parameter of trabecular bone from its 2D projection. Medical Image Analysis 11 (1), 91–98.
Jin, X., Ong, S., Jayasooriah,, 1995. A practical method for estimating fractal dimension. Pattern Recognition Letters 16 (5), 457–464.
John, S., Bradford, A., 1993. The electroencephalogram: Its pattern and origins, MIT Press (Eds), London.
Jun, Y., Yoon, Y., Yoon, H., 1994. ECG data compression using fractal interpolation. Proceedings of the 16th Annual International Conference of the IEEE Engineering in Medicine and Biology Society 1 (3-6), 161-162.
Kalmanti, E., Maris, T.G., 2007. Fractal dimension as an index of brain cortical changes throughout life. In Vivo 21 (4), 641–646.
Kaplan, L., 1999. Extended fractal analysis for texture classification and segmentation. IEEE Transactions on Image Processing 8 (11), 1572–1585.
Kedzia, A., Rybaczuk, M., Andrzejak, R., 2002. Fractal dimensions of human brain cortex vessels during the fetal period. Medical Science Monitor 8 (3), 46–51.
Keller, J., Crownover, R., Chen, S., 1989. Texture description and segmentation through fractal geometry. Computer Vision Graphics and Image Processing 45 (2), 150–160.
Kenkel, N., Walker, D., 1996. Fractals in the biological sciences. Coenoses 1, 77–100.
Keough, K., Hyam, P., Pink, D., Quinn, B., 1991. Cell surfaces and fractal dimensions. Journal of Microscopy 163 (1), 95–99.
Kestener, P., Arneodo, A., 2003. A three-dimensional wavelet based multifractal method : about the need of revisiting the multifractal description of turbulence dissipation data. Physical Review Letter 91 (19), 194501.1–194501.4.
Kestener, P., Lina, J., Saint-Jean, P., Arneodo, A., 2004. Wavelet-based multifractal formalism to assist in diagnosis in digitized mammograms. Image Analysis and Stereology 20 (3), 169–175.
Khalil, A., Joncas, G., Nekka, F., Kestener, P., Arneodo, A., 2006. Morphological analysis of H I features. II. Wavelet-based multifractal formalism. Astrophysical Journal 165 (2), 512–550.
Khosrovi, P., Kahn, A., Genant, H., Majumdar, S., 1994. Characterization of trabecular bone structure from radiographs using fractal analysis. Journal of Bone and Mineral Research 9, 156–157.
Kikuchi, A., Unno, N., Horikoshi, T., Shimizu, T., Kozuma, S., Taketani, Y., 2005. Changes in fractal features of fetal heart rate during pregnancy. Early Human Development 81, 655–661.
Klapetek, P., Ohlidal, I., 2005. Applications of the wavelet transform in AFM data analysis. Acta Physica Slovaca 55 (3), 295–303.
Klinkenberg, B., Goodchild, M., 1992. The fractal properties of topography: a comparison of methods. Earth Surface Processes and Landforms 17, 217–234.
Kolibal, J., Monde, J., 1998. Fractal image error analysis. Computers & Geosciences 4 (8), 785–795.
Kolmogorov, A., 1941. The local structure of turbulence in incompressible viscous fluid for very large reynolds number. Comptes Rendus de l'Académie des sciences 30, 9–13.
Krenz, G., Linehan, J., Dawson, C., 1992. A fractal continuum model of the pulmonary arterial tree. Journal of Applied Physiology 72 (6), 2225–2237.
Kulish, V., Sourin, A., Sourina, O., 2006. Human electroencephalograms seen as fractal time series: Mathematical analysis and visualization. Computers in Biology and Medicine 36, 291–302.
Lam, N., De Cola, L., 2002. Fractals in Geography. The Blackburn Press (Eds), Caldwell, NJ, 308 pp.
Lam, N., Qiu, H., Quattochi, D., 1997. An evaluation of fractal surface measurement methods using ICAMS (Image Characterization and Modeling System). ACSM/ASPRS Annual Convention 5, 377–386.
Lam, N., Qiu, H., Quattochi, D., Emerson, C., 2002. An evaluation of fractal methods for characterizing image complexity. Cartography and Geographic Information Science 29 (1), 25–35.
Landini, G., Rippin, J.W., 1996. Quantification of nuclear pleomorphism using an asymptotic fractal model. Analytical & Quantitative Cytology & Histology 18 (2), 167–176.
Lanyi, M., 1986. Diagnosis and differential diagnosis of breast calcifications. Springer-Verlag (Eds), Berlin, Heidelberg, New York, 252 pp.
Lashermes, B., Jaffard, S., Abry, P., 2005. Wavelet leader based multifractal analysis. Acoustics, Speech, and Signal Processing 4 (18), 161–164.
Lee, W., Chen, Y., Chen, Y., Hsieh, K., 2005. Unsupervised segmentation of ultrasonic liver images by multiresolution fractal feature vector. Information Sciences 175 (3), 177–199.
Lespessailles, E., Jullien, A., Eynard, E., Harba, R., Jacquet, G., Ildefonse, J., Ohley, W., Benhamou, C.L., 1998. Biomechanical properties of human os calcanei: relationships with bone density and fractal evaluation of bone microarchitecture. Journal of Biomechanics 31 (9), 817–824.
Lévy-Véhel, J., 1995. Fractal approches in signal processing. Fractals 3, 755–775.
Lévy-Véhel, J., Mignot, P., Berroir, J., 1992. Texture and Multifractals: New tools for image analysis. Technical report of INRIA-Rocquencourt, vol. 1706.
Lévy-Véhel, J., Vojak, R., 1995. Multifractal analysis of Choquet capacities: Preliminary Results. Technical report of INRIA-Rocquencourt, vol. 2576.
Li, H., Liu, K., Lo, S., 1996. Enhancement of micro-calcifications on mammograms using a fractal modelling approach. Proceedings of the 18th Annual International Conference of the IEEE Engineering in Medecine and Biology Society 3, 1111-1112.
Li, H., Giger, M.L., Olopade, O.I., Lan, L., 2007. Fractal analysis of mammographic parenchymal patterns in breast cancer risk assessment. Academic Radiology 14 (5), 513–521.
Li, X., Polygiannakis, J., Kapiris, P., Peratzakis, A., Eftaxias, K., Yao, X., 2005. Fractal spectral analysis of pre-epileptic seizures in terms of criticality. Journal of Neural Engineering 2 (2), 11–16.
Link, T., Majumdar, S., Konermann, W., Meier, N., Lin, J., Newitt, D., Ouyang, X., Peters, P., Genant, H., 1997. Texture analysis of direct magnification radiographs of vertebral specimens: correlation with bone mineral density and biomechanical properties. Academic Radiology 4, 167–176.
Liu, J., Zhang, L., Yue, G., 2003. Fractal dimension in human cerebellum measured by magnetic resonance imaging. Biophysical Journal 85 (6), 4041–4046.
Lopes, R., Betrouni, N., Szurhaj, W., Steinling, M., 2007a. 3D Fractal analysis for epilepsy characterization on SPECT images. European Journal of Nuclear Medicine 34 (2), 394.
Lopes, R., Dubois, P., Dewalle, A., Maouche, S., Betrouni, N., 2007b. 3D multifractal analysis of cerebral tomoscintigraphy images. International journal of Computer Assisted Radiology and Surgery 2 (Supp1), 17–18.
Lopes, R., Dubois, P., Makni, N., Szurhaj, W., Maouche, S., Betrouni, N., 2008. Classification of brain SPECT imaging using 3D local multifractal spectrum for epilepsy detection. International Journal of Computer Assisted Radiology and Surgery 3 (3-4), 341–346.
Maeda, J., Novianto, S., Miyashita, A., Saga, S., Suzuki, Y., 1998. Fuzzy region-growing segmentation of natural images using local fractal dimension. Proceedings of the 14th International Conference on Pattern Recognition 2, 991.
Majumdar, S., Lin, J., Link, T., Millard, J., Augat, P., Ouyang, X., Newitt, D., Gould, R., Kothari, M., Genant, H., 1999. Fractal analysis of radiographs: Assessment of trabecular bone structure and prediction of elastic modulus and strength. Medical Physics 26 (7), 1330–1340.
Mandelbrot, B., 1963. The variation of certain speculative prices. J. of Business 36, 394–419.
Mandelbrot, B., 1975. Les objets fractals : forme, hasard et dimension. Flammarion (Eds), Paris, 208 pp.
Mandelbrot, B., 1977. Fractals: Form. Chance and Dimension, Freeman (Eds), 365 pp.
Mandelbrot, B., 1983. The Fractal Geometry of Nature. Freeman (Eds), 468 pp.
Mandelbrot, B., 1967. How long is the coast of Britain? Statistical self-similarity and fractional dimension. Science 156, 636–638.
Mandelbrot, B., 1985. Self-affine fractals and the fractal dimension. Physica Scripta 32, 257–260.
Mansury, Y., Deisboeck, T., 2004. Simulating "structure-function" patterns of malignant brain tumors. Physica A 331 (1–2), 219–232.

Martinez, P., Schertzer, D., Pham, K., 1997. Texture modelisation by multifractal processes for SAR image segmentation. Radar 97 (4), 135–139.
Mavroforakis, M., Georgiou, H., Dimitropoulos, N., Cavouras, D., Theodoridis, S., 2006. Mammographic masses characterization based on localized texture and dataset fractal analysis using linear, neural and support vector machine classifiers. Artificial Intelligence In Medicine 37, 145–162.
Messent, E., Ward, R., Tonkin, C., Buckland-Wright, C., 2005. Tibial cancellous bone changes in patients with knee osteoarthritis. A short-term longitudinal study using fractal signature analysis. OsteoArthritis and Cartilage 13, 463–470.
Meyer, Y., 1998. Wavelets, vibrations and scaling. CRM Monograph Ser. 9, American Mathematical Society, Providence, RI.
Molteno, T., 1993. Fast O(N) box-counting algorithm for estimating dimensions. Physical Review E 48 (5), 3263–3266.
Munoz, D.A., Angulo, B.F., Del Rio Correa, J.L., 2005. Changes in multifractality with aging and heart failure in heartbeat interval time series. Proceedings of the 29th Annual International Conference of the IEEE Engineering in Medicine and Biology Society 7, 6981-6984.
Murali, S., 2005. Fractal and FFT power spectra analysis of human electroencephalograms (brain waves) for six different odors, M.Sc. dissertation, Nanyang Technological University, Singapore.
Nagao, M., Murase, K., 2002. Measurement of heterogeneous distribution on Technegas SPECT images by three-dimensional fractal analysis. Annals of Nuclear Medicine 16 (6), 369–376.
Nguyen, T., Rangayyan, R., 2005. Shape Analysis of Breast Masses in Mammograms via the Fractal Dimension. Proceedings of the 29th Annual International Conference of the IEEE Engineering in Medecine and Biology Society 3, 3210-3213.
Normant, F., Tricot, C., 1991. Methods for evaluating the fractal dimension of curves using convex hulls. Physical Review A 43 (12), 6518–6525.
Novianto, S., Suzuki, Y., Maeda, J., 2003. Near optimum estimation of local fractal dimension for image segmentation. Pattern Recognition Letters 24 (1–3), 365–374.
Oczeretko, E., Juczewska, M., Kasacka, I., 2001. Fractal geometric analysis of lung cancer angiogenic patterns. Folia Histochemica et Cytobiologica 39 (Suppl. 2), 75–76.
Oiwa, N., Glazier, J., 2004. Self-Similar Mitochondrial DNA. Cell. Biochem. Biophys. 41 (1), 41–62.
Osborne, A.R., Provenzale, A., 1989. Finite correlation dimension for stochastic systems with power-law spectra. Physica D 35, 357–381.
Ott, S., 1986. Should women get screening bone mass measurements? Annals of Internal Medicine 104, 874–876.
Ouyang, X., Majumdar, S., Link, T., Lu, Y., Augat, P., Lin, J., Newitt, D., Genant, H., 1998. Morphometric texture analysis of spinal trabecular bone structure assessed using orthogonal radiographic projections. Medical Physics 25 (10), 2037–2045.
Owis, M., Abou-Zied, A., Youssef, A., Kadah, Y., 2002. Study of features based on nonlinear dynamical modeling in ECG arrhythmia detection and classification. IEEE Transactions on Biomedical Engineering 49 (7), 733–736.
Papaloucas, C., Ward, R., Tonkin, C., Buckland-Wright, C., 2005. Cancellous bone changes in hip osteoarthritis: a short-term longitudinal study using fractal signature analysis. OsteoArthritis and Cartilage 13 (11), 998–1003.
Parkinson, I., Fazzalari, N., 1994. Cancellous bone structure analysis using image analysis. Australasian Physical and Engineering Sciences in Medicine 470, 64–70.
Peleg, S., Naor, J., Hartley, R., Avnir, D., 1984. Multiple resolution texture analysis and classification. IEEE Transactions on Pattern Analysis and Machine Intelligence 6 (6), 661–674.
Penn, A., Bolinger, L., Schnall, M., Loew, M., 1999. Discrimination of MR images of breast masses with fractal-interpolation function models. Academic Radiology 6 (3), 156–163.
Pentland, A., 1984. Fractal-based description of natural scenes. IEEE Transactions on Pattern Analysis and Machine Intelligence 6 (6), 661–674.
Pereda, E., Gamundi, A., Rial, R., Gonzalez, J., 1998. Non-linear behaviour of human EEG: fractal exponent versus correlation dimension in awake and sleep stages. Neuroscience Letters 250 (2), 91–94.
Pereira, D., Zambrano, C., Martin-Landrove, M., 2000. Evaluation of malignancy in tumors of the central nervous system using fractal dimension. Proceedings of the 22nd Annual International Conference of the IEEE Engineering in Medicine and Biology Society 3, 1775-1778.
Perrier, E., Tarquis, A., Dathe, A., 2006. A program for fractal and multifractal analysis of 2D binary images : Computer algorithms versus mathematical theory. Geoderma 134 (3–4), 284–294.
Pham, D., Xu, C., Prince, J., 1999. Current methods in medical image segmentation. Annual Review of Biomedical Engineering 2, 315–337.
Phothisonothai, M., Nakagawa, M., 2007. Fractal-based EEG data analysis of body parts movement imagery tasks. Journal of Physiological Sciences 57 (4), 217–226.
Pickover, C., Khorasani, A., 1986. Fractal characterization of speech waveforms graphs. Computer Graphics 1 (1), 51–61.
Popivanov, D., Jivkova, S., Stomonyakov, V., Nicolova, G., 2005. Effect of independant component analysis on multifractality of EEG during visual-motor task. Signal Processing 85 (11), 2112–2123.
Pratt, W., Faugeras, O., Gagalowicz, A., 1978. Visual discrimination of stochastic texture fields. IEEE Transactions on Systems. Man and Cybernetics 8 (11), 796–804.
Prigarin, S., Hahn, K., Winkler, G., 2008. Comparative analysis of two numerical methods to measure Hausdorff dimension of the fractional Brownian motion. Numerical Analysis and Applications 1 (2), 163–178.
Pruess, S., 2007. Some remarks on the numerical estimation of fractal dimension. In: Fractals in the Earth Sciences, C.C. Barton and P.R. La Pointe, Plenum Press (Eds), New-York, Chap. 3, 65–75.
Qiu, H., Lam, N., Quattochi, D., Gamon, J., 1999. Fractal characterization of hyperspectral imagery. Photogrammetric Engineering and Remote Sensing 65 (1), 63–71.
Rangayyan, R., Nguyen, T., 2005. Pattern classification of breast masses via fractal analysis of their contours. Proceedings of Computer Assisted radiology and Surgery (CARS) 1281, 1041–1046.
Renyi, A., 1955. On a new axiomatic theory of probability. Acta Mathematica Hungarica 6 (3–4), 285–335.
Russel, D., Hanson, J., Ott, E., 1980. Dimension of strange attractors. Physical Review Letters 45 (14), 1175–1178.
Ruttiman, U., Webber, R., Hazelrig, J., 1992. Fractal dimension from radiographs of peridental alveolar bone. Oral Pathology 74 (1), 98–110.
Rybaczuk, M., Kedzia, A., Blaszcyk, E., 1996. Fractal description of cerebellum surface during fetal period. Folia Morphologica 55 (4), 434–436.
Sandau, K., Kurz, H., 1997. Measuring fractal dimension and complexity–an alternative approach with an application. Journal of Microscopy 186 (2), 164–176.
Sanderson, B., Goulding, A., 1990. The fractal dimension of relative Lagrangian motion. Tellus 42A, 550–556.
Sato, K., Sugawara, K., Narita, Y., Namura, I., 1996. Consideration of the method of image diagnosis with respect to frontal lobe antrophy. Proceedings of IEEE Transactions on Nuclear Science 43, 3230–3239.
Shan, Z., Liu, J., Glass, J., Gajjar, A., Li, C., Reddick, W., 2006. Quantitative morphological evaluation of white matter in survivors of chilhood medulloblastoma. Magnetic Resonance Imaging 24 (8), 1015–1022.
Shelberg, M., Lam, N., Moellering, H., 1983. Measuring the fractal dimension of surfaces. Proceedings of the Sixth International Symposium on Computer-Assisted Cartography Auto-Carto 6, 319–328.
Shimizu, Y., Barth, M., Windischberger, C., Moser, E., Thurner, S., 2004. Wavelet-based multifractal analysis of fMRI time series. NeuroImage 22 (3), 1195–1202.
Sisodiya, S., Free, S., 1997. Disproportion of cerebral surface areas and volumes in cerebral dysgenesis. MRI-based evidence for connectional abnormalities. Brain 120 (2), 271–281.
Small, M., Yu, D., Harrison, R., Grubb, N., Fox, K., 2002. Uncovering non-linear structure in human ECG recordings. Chaos, Solitons & Fractals 13, 1755–1762.
Smith, T., Behar, T., 1994. Comparative fractal analysis of cultured glia derived from optic nerve and brain demonstrate different rates of morphological differentiation. Brain Research 634 (2), 181–190.
Smith, T., Brauer, K., Reichenbach, A., 1993. Quantitative phylogenetic constancy of cerebellar Purkinje cell morphological complexity. The Journal of Comparative Neurology 331 (3), 402–406.
Smrcka, P., Bittner, R., Vysoky, P., Hana, K., 2003. Fractal and multifractal properties of heartbeat interval series in extremal states of the human organism. Measurement Science Review 3, 13–15.
Soille, P., Rivest, J., 1996. On the validity of fractal dimension measurements in image analysis. Journal of Visual Communication and Image Representation 7 (3), 217–229.
Soltys, Z., Ziaja, M., Pawlinski, R., Setkowicz, Z., Janeczko, K., 2001. Morphology of reactive microglia in the injured cerebral cortex. Fractal analysis and complementary quantitative methods. Journal of Neuroscience Research 63 (1), 90–97.
Spasic, S., Kalauzi, A., Grbic, G., Martac, L., Culic, M., 2005. Fractal analysis of rat brain activity after injury. Medical and Biological Engineering and Computing 43 (3), 345–348.
Stojic, T., Reljin, I., Reljin, B., 2006. Adaptation of multifractal analysis to segmentation of microcalcifications in digital mammograms. Physica A 367, 494–508.
Stosic, T., Stosic, B.D., 2006. Multifractal analysis of human retinal vessels. IEEE Transactions on Medical Imaging 25 (8), 1101–1107.
Sun, W., 2006. Three new implementations of the triangular prism method for computing the fractal dimension of remote sensing images. Photogrammetric Engineering and Remote Sensing 72 (4), 373–382.
Suri, J., Setarehdan, S., Sing, S., 2002. Advanced algorithmic approaches to medical image segmentation, Springer (Eds), New-York, 668 pp.
Tabar, L., Duffy, S., Burhenne, L., 1993. New Swedish breast cancer detection results for women aged 40–49. Cancer 72 (suppl. 4), 1437–1448.
Takahashi, T., Murata, T., Narita, K., Hamada, T., Kosaka, H., Omori, M., Takahashi, K., Kimura, H., Yoshida, H., Wada, Y., 2006. Multifractal analysis of deep white matter microstructural changes on MRI in relation to early-stage atherosclerosis. NeuroImage 32 (3), 1158–1166.
Taleb-Ahmed, A., Dubois, P., Duquenoy, E., 2003. Analysis methods of CT-scan images for the characterization of the bone texture: First results. Pattern Recognition Letters 24 (12), 1971–1982.
Tanki, N., Murase, K., Nagao, M., 2006. A new parameter enhancing breast cancer detection in computer-aided diagnosis of X-ray mammograms. Igaku Butsuri 26 (4), 207–215.
Taylor, P., Hajnal, S., Dilhuydy, M., Barreau, B., 1994. Measuring image texture to separate ‘‘difficult” from ‘‘easy” mammograms. British Journal of Radiology 67, 456–463.

Tél, T., Fulop, A., Vicsek, T., 1989. Determination of fractal dimensions for geometrical multifractals. Physica A 159, 155–166.
Thakor, N., Zhu, Y., Pan, K., 1990. Ventricular tachycardia and fibrillation detection by a sequential hypothesis testing algorithm. IEEE Transactions on Biomedical Engineering 37 (9), 837–843.
Thompson, P., Schwartz, C., Lin, R., Khan, A., Toga, A., 1996. Three-dimensional statistical analysis of sulcal variability in the human brain. Journal of Neuroscience 16 (13), 4261–4274.
Touchette, H., Beck, C., 2005. Nonconcave entropies in multifractals and the thermodynamic formalism. Journal of Statistical Physics 125 (2), 455–471.
Tourassi, G., 1999. Journey toward computer-aided diagnosis: Role of image texture analysis. Radiology 213 (2), 317–320.
Uitewaal, P., Lips, P., Netelenbos, J., 1987. An analysis of bone structure in patients with hip fracture. Journal of Bone and Mineral Research 3 (2), 63–67.
Veldkamp, W., Karssemeijer, N., Otten, J., Hendriks, J., 2000. Automated classification of clustered microcalcifications into malignant and benign types. Medical Physics 27 (11), 2600–2608.
Veneziano, D., Moglen, G., Bras, R., 1995. Multifractal analysis: pitfalls of standard procedures and alternatives. Physical Review E 52 (2), 1387–1398.
Vicsek, T., 1990. Mass multifractals. Physica A 168, 490–497.
Wang, G., Huang, H., Xie, H., Wang, Z., Hu, X., 2007. Multifractal analysis of ventricular fibrillation and ventricular tachycardia. Medical Engineering & Physics 29 (3), 375–379.
Wang, G., Ren, X., Li, L., Wang, Z., 2006. Multifractal analysis of surface EMG signals for assessing muscle fatigue during static contractions. Journal of Zhejiang University - Science A 8, 910–915.
Wang, J., Ning, X., Ma, Q., Bian, C., Xu, Y., Chen, Y., 2005. Multiscale multifractality analysis of a 12-lead electrocardiogram. Physical Review E 71 (6), 062902.1–062902.4.
Wax, A., Yang, C., Muller, M., Nines, R., Boone, C., Steele, V., Stoner, G., Dasari, R., Feld, M., 2003. In situ detection of neoplastic transformation and chemopreventive effects in rat esophagus epithelium using angle-resolved low-coherence interferometry. Cancer Research 63, 3556–3559.
Wilkie, J.R., Giger, M.L., Chinander, M.R., Vokes, T.J., Li, H., Dixon, L., Jaros, V., 2004. Comparison of radiographic texture analysis from computed radiography and bone densitometry systems. Medical Physics 31 (4), 882–891.
Woyshville, M., Calabrese, J., 1994. Quantification of occipital EEG changes in Alzheimer's disease utilizing a new metric; the fractal dimension. Biological Psychology 35 (6), 291–302.
Xia, Y., Feng, D., Zhao, R., 2006. Morphology-based multifractal estimation for texture segmentation. IEEE Transactions on Image Processing 15 (3), 614–624.
Yasar, F., Akgunlu, F., 2006. The differences in panoramic mandibular indices and fractal dimension between patients with and without spinal osteoporosis. Dentomaxillofacial Radiology 35 (1), 1–9.
Yi, W.J., Heo, M.S., Lee, S.S., Choi, S.C., Huh, K.H., Lee, S.P., 2007. Direct measurement of trabecular bone anisotropy using directional fractal dimension and principal axes of inertia. Oral surgery, oral medicine, oral pathology, oral radiology, and endodontics 104 (1), 110–116.
Yoshikawa, T., Murase, K., Oku, N., Kitagawa, K., Imaizumi, M., Takasawa, M., Nishikawa, T., Matsumoto, M., Hatazawa, J., Hori, M., 2003. Statistical Image Analysis of Cerebral Blood Flow in Vascular Dementia with Small-Vessel Disease. Journal of Nuclear medicine 44 (4), 505–511.
Yu, Z.G., Anh, V., Lau, K.S., 2001. Measure representation and multifractal analysis of complete genomes. Phys. Rev. E Stat. Nonlin. Soft Matter Physics 64, 031903.
Yum, M.K., Kim, J.S., 2002. Increased intermittency and decreased nonstationarity of heart rates during the daytime in patients with neurocardiogenic syncope. Journal of Cardiovascular Electrophysiology 13 (8), 788–793.
Zhang, H., Zhu, Y.S., Xu, Y., 2002. Complexity information based analysis of pathological ECG rythm for ventricular tachycardia and ventricula fibrillation. International Journal of Bifurcation and Chaos 12, 2293–2303.
Zhang, L., Dean, D., Liu, J., Sahgal, V., Wang, X., Yue, G., 2006. Quantifying degeneration of white matter in normal aging using fractal dimension. Neurobiology of Aging 28 (10), 1543–1555.
Zhang, X.S., Zhu, Y.S., Thakor, N.V., Wang, Z.Z., 1999. Detecting ventricular tachycardia and fibrillation by complexity measure. IEEE Transactions on Biomedical Engineering 46 (5), 548–555.
Zhuang, X., Meng, Q., 2004. Local fuzzy fractal dimension and its application in medical image processing. Artificial Intelligence in Medicine 32 (1), 29–36.
Zook, J., Iftekharuddin, K., 2005. Statistical analysis of fractal-based brain tumor detection algorithms. Magnetic Resonance Imaging 23 (5), 671–678.